ENCLOSURE 4

GEH Technical Report

002N8467 Revision 4

Fuel Rack Seismic Analysis

HITACHI

GE Hitachi Nuclear Energy

3901 Castle Hayne Road
Wilmington, NC
28401

002N8467
Revision 4
Class I
April 2016

NORTH ANNA 3 FUEL RACK SEISMIC ANALYSIS

IMPORTANT NOTICE REGARDING CONTENTS OF THIS REPORT

Please read carefully

The information contained in this document is furnished for the purpose of supporting the NRC review of the North Anna 3 ESBWR. The only undertakings of GE-Hitachi Nuclear Energy (GEH) with respect to information in this document are contained in contracts between GEH and any participating utilities, and nothing contained in this document shall be construed as changing those contracts. The use of this information by anyone other than that for which it is intended is not authorized; and with respect to any unauthorized use, GEH makes no representation or warranty, and assumes no liability as to the completeness, accuracy, or usefulness of the information contained in this document.

TABLE OF CONTENTS

1. INTRODUCTION 1
1.1 Purpose 1
1.2 Scope 1
2. SPENT FUEL RACKS IN THE SPENT FUEL POOL 3
2.1 Analysis Summary 3
2.2 Seismic Demand 6
2.3 Results 11
3. SPENT FUEL RACKS IN THE BUFFER POOL DEEP PIT 21
3.1 Analysis Summary 21
3.2 Seismic Demand 24
3.3 Results 28
3.4 Design Changes 29
4. NEW FUEL RACKS IN THE BUFFER POOL 38
4.1 Analysis Summary 38
4.2 Seismic Demand 41
4.3 Results 42
4.4 Design Changes 43
5. CONCLUSION 51
6. REFERENCES 52

1. INTRODUCTION

1.1 Purpose

The structural integrity of the ESBWR fuel racks are evaluated for DCD plant conditions in Reference 1. Question 03.07.02-20 of Request for Additional Information 123 (Reference 2) identifies North Anna 3 (NA3) site-specific exceedances in the Safe Shutdown Earthquake (SSE) response spectra at the locations of the fuel racks and requests an assessment of the structural design of these racks using site-specific SSE seismic demands.

The ESBWR design utilizes three fuel rack designs: spent fuel pool fuel storage racks (FSR), buffer pool deep pit FSR, and buffer pool new FSR. Assessments have been performed for each of these fuel rack designs using the guidance provided in Appendix D of NRC Standard Review Plan (SRP) Section 3.8.4 ("Guidance on Spent Fuel Pool Racks"). The purpose of this report is to summarize the structural assessments of all three FSR designs. Additionally, for those components of the individual fuel racks that are overstressed resulting from increased seismic demand, a description of the design changes are provided.

1.2 Scope

This document only provides a summary of the maximum enveloping results from the site-specific assessments of the FSR as well as comparisons of the site-specific seismic demand to the ESBWR DCD seismic demand. The full analyses of the FSR can be found in Reference 3, Reference 4 and Reference 5 for the spent fuel pool FSR, buffer pool deep pit FSR, and the buffer pool new FSR, respectively.

The structural evaluation of the fuel assemblies enclosed in the FSR is not within the scope of this document. The fuel assemblies are qualified for the NA3 site-specific seismic demand in Reference 6.

The structural evaluations of the pool liners and anchorage embedment designs are outside of the scope of this report. However, the loads on the pool liner are provided for free standing racks (spent fuel pool FSR) and the anchor embedment loads are provided for anchored racks (buffer pool deep pit FSR and buffer pool new FSR).

The load drop impact analysis and thermal hydraulic analysis contained in Section 4.0 and 5.0 of Reference 1 are not considered as these evaluations are unaffected by seismic demands.

Section 2.0 of this report contains a summary of the results of the NA3 SSE site-specific seismic evaluation of the spent fuel pool FSR.

Section 3.0 contains a summary of the results of the NA3 SSE site-specific seismic evaluation of the buffer pool deep pit FSR. The design changes of these racks and the justification for the adequacy of these changes for the ESBWR DCD seismic demands are contained in Section 3.4.

Section 4.0 contains a summary of the results of the NA3 SSE site-specific seismic evaluation of the buffer pool new FSR. The design changes of these racks and the justification for the adequacy of these changes for the ESBWR DCD seismic demands are contained in Section 4.4.

2. SPENT FUEL RACKS IN THE SPENT FUEL POOL

The structural adequacy of the FSR in the spent fuel pool to the ESBWR DCD seismic demands was demonstrated in Section 1.0 of Reference 1. To ensure the structural adequacy of the FSR in the spent fuel pool for the seismic demands of NA3, the analysis documented in Section 1.0 of Reference 1 was repeated using the NA3 site-specific SSE acceleration response spectra. This analysis is contained in Reference 3.

A brief summary of the structural assessment is provided in Section 2.1. The information contained in Section 2.1 is a repeat of information provided in the ESBWR DCD spent fuel pool FSR report (Section 1.0 of Reference 1) as an aide for understanding the current, site-specific evaluation of these racks. The site-specific seismic demand for these racks is discussed in Section 2.2 along with a discussion of the statistical independence of the input time histories and the potential impact on the results of the qualification. The maximum enveloping results of the assessment including stress results, displacements, and loads on the fuel pool liner are provided in Section 2.3.

2.1 Analysis Summary

The spent fuel pool FSR are qualified using guidance from Appendix D of SRP Chapter 3.8.4. The following is a brief description of the site-specific seismic evaluation of the spent fuel pool FSR. See Reference 3 for the assessment in its entirety.

Overview

The spent fuel racks in the spent fuel pool are designed to support and protect the spent fuel assemblies. They are made of stainless steel and borated stainless steel plates, forming 15x12 (or 14x12) cells to house the spent fuel assemblies. The spent fuel pool racks are supported on four bottom-corner cylindrical feet, each of which rests on a bearing pad shared by the feet of adjacent racks. The spent fuel pool racks are free to slide and are only supported by their own weight and friction between the bearing pads and the pool liner. Upper link crossarms connect adjacent racks at the upper corners.

To analyze these racks both a Response Spectrum Analysis (RSA) and transient analysis are performed to ensure the structural adequacy of the individual components responsible for maintaining the adequacy of the spent fuel pool FSR.

Design Code

The spent fuel pool FSR are designed to the stress limits of ASME Boiler and Pressure Vessel (B&PV) Code, Section III, Division 1, Subsection NF requirements for Class 3 component supports (Reference 7).

Loads and Combinations

The load combinations affected by the change in seismic demand are shown in this section; all other load combination results are unaffected. The load combination for the RSA is provided in Eq. (1) and Eq. (2) for the transient analysis.

Level D:	$D + SSE + SRVD + LOCA + T_a$ (RSA)	(1)
Level D:	$D + SSE + T_a$ (transient dynamic analysis)	(2)[1]

The dead weight (D) is evaluated as a static load under the effect of gravity. The SSE, Safety Relief Valve Discharge (SRVD), and Loss-of-Coolant Accident (LOCA) are all dynamic loads acting at the base of the rack. There are no thermal (T_a) loads on the structure because sufficient clearance is provided for thermal expansion; however, the thermal displacement is considered in determining the potential impact with the pool wall.

Analysis Procedure

The analysis of the racks is divided into two calculation stages which both utilize the finite element program ANSYS 10.0. A RSA is used to calculate global loads

[1] Only the SSE effects are evaluated in the transient analysis. There is no licensing basis for combining LOCA and SSE loads in Appendix D of SRP 3.8.4.

on the structure and a non-linear transient analysis is used to determine the impact loads between structures as well as the maximum displacements.

Analysis Procedure (RSA)

A detailed finite element model of a single spent fuel pool rack is developed using shell and lumped mass elements. The structural response to the dead load is determined by static analysis. The dynamic loads are determined by RSA using the first 100 modes up to 185.4 Hz. The site-specific response spectra are discussed in Section 2.2. Consistent with NRC Regulatory Guide 1.92, the modal responses for a given dynamic load in each direction are combined using the grouping method and the resulting spatial components are combined by Square Root of the Sum of Squares (SRSS). The effects of missing mass in the RSA are accounted for using pseudo-static evaluation consistent with Appendix A of Reg. Guide 1.92.

The results of the RSA are used to determine overall stresses at the critical locations of the rack's components. These are combined, as appropriate, with the impact stresses resulting from the transient analysis.

Analysis Procedure (Transient Analysis)

Synthesized site-specific acceleration time histories are converted to displacements by double integration and used as base input motion to a global model containing 20 simplified FSR models each composed of beam and lumped mass elements. The global model simulates contact, hydrodynamic coupling and link conditions between the individual freestanding racks. This time history analysis was performed for 16 seconds using 0.005 second intervals. Rayleigh proportional damping is used which provides effective damping below 4% of critical damping across the 2 Hz to 53 Hz frequency band which was deemed the most significant. The displacement time-histories for each direction are applied simultaneously at the nodes representing the pool floor and walls. See Section 2.2 for additional information pertaining to the finite element models used for the spent fuel pool FSR analysis as part of a discussion on the statistical independence of the time history inputs.

The time history analysis is performed for six scenario-cases which vary the fuel assembly fill levels and bearing pad friction for individual racks. This analysis is used to generate relative displacements, reactions, and transmission forces which are bounded across the scenario cases. From the six scenario-cases the enveloping forces, moments and displacements are extracted.

The spent fuel pool rack local stresses are then calculated based on the maximum impact forces evaluated in the transient analysis. The maximum impact forces are applied at the top of the rack and at the rack base plate in both tension and compression resulting in four impact load cases. The maximum stresses across the four impact load cases are used in the final stress evaluation. In addition, the peak global bending moment on the rack is used to generate a scaling factor, f_M, equal to the ratio of the peak global moment from the transient analysis to the peak moment from the RSA. The scaling factor is used to reduce the conservatisms in the RSA and is discussed in detail in Section 8 of Reference 3.

The impact stresses are combined with the scaled stresses generated in the RSA to generate the limiting stresses that are then evaluated using ASME Code Section III, Division 1, Subsection NF acceptance criteria.

2.2 Seismic Demand

The NA3 site-specific response spectra for the ESBWR fuel racks are provided in a site-specific design specification data sheet for the fuel racks (Reference 8). The NA3 response spectra for the spent fuel pool racks documented in Reference 8 are taken from the Node 2 results of the site-specific bounding SSE demands from Reference 9. Node 2 represents the base slab which the spent fuel pool rests on. All spectra for the fuel racks are taken at 4% damping consistent with Reg. Guide 1.61 for welded steel structures for SSE analysis.

The NA3 spent fuel pool FSR response spectra are shown with comparisons to the DCD response spectra in Figure 1, Figure 2, and Figure 3 for the plant North-

South, East-West and Vertical direction, respectively[2]. The DCD response spectra are retrieved from Section 1.0 of Reference 1.

The analysis of the spent fuel racks requires synthesized acceleration time histories in addition to the response spectra. The time histories are used in a non-linear transient analysis to determine the dynamic behavior of the freestanding spent fuel pool FSR (see Section 2.1 for further discussion). The synthesized acceleration time histories for the spent fuel pool FSR are documented in Reference 10. Reference 10 demonstrates that the response spectra generated in each of the 3 orthogonal directions sufficiently envelops the design spectra.

The cross-correlation coefficients between the synthesized time histories are provided in Reference 10 and repeated here:

N-S & E-W - 0.18

E-W & Vertical - 0.17

N-S & Vertical - 0.24

These cross-correlation coefficients are slightly greater than the 0.16 value allowed in SRP Section 3.7.1 ("Seismic Design Parameters") for a non-linear transient analysis. This could result in a potential non-conservative evaluation of the spent fuel pool FSR. For the spent fuel pool FSR, the time history evaluation is used to generate bounding impact loads and to determine a scaling factor, f_M, for the RSA. The impact of the non-statistically independent time histories is discussed in the following section.

[2] The response spectra are provided from 10 Hz to 200 Hz as the fundamental frequency of the spent fuel pool storage rack is 13.8 Hz and the highest eigenvalue included in the RSA is 185.4 Hz.

Cross-Correlation Coefficient Discussion

The model of the fuel racks used in the spent fuel pool FSR time history evaluation was discussed in Section 2.1 and is shown here.

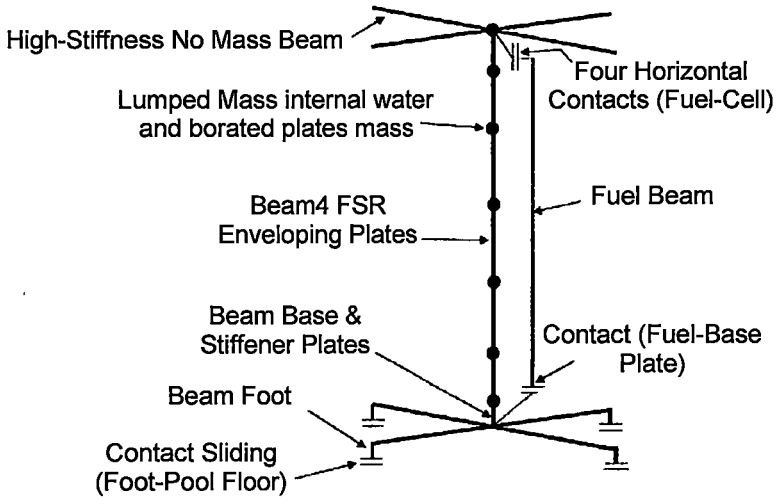

The spent fuel pool FSR model consists of two overlaid beams (shown above as two separated beams for clarity) representing the fuel and the FSR enveloping plate/base. The model is tuned to the approximate natural frequency of the detailed model in both horizontal directions. The fuel beam's lowest node is coupled to the FSR in the horizontal directions and a contact element is used in the vertical direction which allows the fuel to lift off the base plate and then return to impact the base plate. The fuel's uppermost node has horizontal contact elements used to evaluate lateral impacts of the fuel with the upper grid structure of the FSR. Four rigid links at the base are connected to sliding contact elements which model sliding friction and contact with the floor. Upper rigid beams have constraints at the end which are used to simulate the displacement constraints imposed by the spent fuel pool FSR crossarms. Twenty of these simplified models are used in the full time history evaluation to assess the impact loads, displacements and peak global moments.

The impact of non-statistically independent time histories is zero if it can be shown that the response of the structure in each given direction is decoupled from input motion in the other two perpendicular directions. While this model is

not totally decoupled, the vertical arrangement of the FSR/Fuel and the small displacements resulting from excitation mean that there will be little coupling between directional components and so the impact of non-independent time histories will be limited.

The stiffness matrix for an Euler-Bernoulli beam element in a two dimensional plane is given in Eq. (3) (from Reference 11). Notice that there is no coupling between the motion in the axial direction of the beam element (u) and the transverse direction (v). However, if the beams rotate sufficiently, stiffness components would exist that couple the vertical response of the horizontal input and vice versa due to the transformation of the FSR elements coordinate system to the global system.

$$\begin{bmatrix} F_{ui} \\ F_{vi} \\ M_{\theta i} \\ F_{uj} \\ F_{vj} \\ M_{\theta j} \end{bmatrix} = \begin{bmatrix} X & 0 & 0 & -X & 0 & 0 \\ 0 & Y_1 & -Y_2 & 0 & -Y_1 & -Y_2 \\ 0 & -Y_2 & Y_3 & 0 & Y_2 & Y_4 \\ -X & 0 & 0 & X & 0 & 0 \\ 0 & -Y_1 & Y_2 & 0 & Y_1 & Y_2 \\ 0 & -Y_2 & Y_4 & 0 & Y_2 & Y_3 \end{bmatrix} \begin{Bmatrix} u_i \\ v_i \\ \theta_i \\ u_j \\ v_j \\ \theta_j \end{Bmatrix} \quad (3)$$

Where: $X = \frac{AE}{L}$ $Y_1 = \frac{12EI}{L^3}$ $Y_2 = \frac{6EI}{L^2}$ $Y_3 = \frac{4EI}{L}$ $Y_4 = \frac{2EI}{L}$

And:

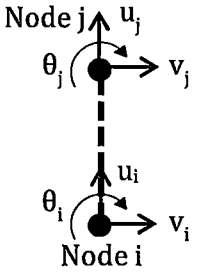

To estimate the amount of overturning in the fuel, θ_T, the maximum relative horizontal displacements of the top of the rack (3.4 mm shown in Table 1) is added to the largest displacement of the fuel relative to the rack (10 mm shown in Table 1). The length of the fuel is roughly 3.5 m. Thus, for a maximum relative displacement of the fuel in the rack of 13.4 mm the angle of rotation is of the fuel is small as shown in Eq. 4.

$$\theta_T = tan^{-1}\left(\frac{0.0134\,m}{3.5\,m}\right) = 0.22° \quad (4)$$

Any rotational transformation of the stiffness matrix by θ_T would result in limited coupling between the horizontal input of the rack and the vertical response of the fuel. Additionally, as moments are not transferred from the fuel racks to the fuel, there is no coupling between the rotation of the FSR and the fuel's response. Thus, for this model the vertical and horizontal responses can be considered practically decoupled.

A similar justification exists between the input in one horizontal direction and the response in the other horizontal direction as the 3-Dimensional beam equations don't have coupling terms between them when the local and global coordinate systems are aligned. Coupling terms will only exist if the fuel experiences rotation about the vertical direction. However, the fuel beam is axisymmetric and torsional moments aren't transferred from the FSR to the fuel so no fuel rotation about the vertical direction occurs. Thus, the horizontal inputs are decoupled and there is no effect of cross-correlation coefficient exceedances between the horizontal direction input and perpendicular response of the fuel.

To justify any small exceedances in cross-correlation coefficients, a review of the conservatisms in the calculation is included next. Following that discussion, the potential impact of increasing the factor, f_M, used to scale the RSA results to a limiting value of 1 are addressed to bound the impact of the cross-correlation coefficient exceedances on the RSA results.

To bound the stresses resulting from impact, peak impact loads are generated from six cases which repeat the transient analysis of the racks while varying the coefficients of friction between the FSR feet and the pool liner. The peak loads are assumed to occur on all four sides of the FSR and are applied as static loads to a linear, detailed model of the FSR to generate component stresses. The simultaneous application of peak loads on all four side of the FSR and the use of linear analysis are both conservative assumptions.

The use of the scaling factor, f_M, for the site-specific evaluation to scale down the RSA analysis stresses may be non-conservative if the impact loads were to increase. While, it is not reasonable to expect a significant increase in impact

loads, as discussed above, the potential impact of an increase is evaluated by increasing the scaling factor. The upper limit for the scaling factor is 1 which represents no adjustment to the RSA results to account for the conservatism of allowing moments to develop between the feet of the FSR and the pool liner by fixing the feet in the RSA. A scaling factor of 1 represents at most a 10% increase in stresses resulting from the RSA. Table 2 contains the limiting component stresses and associated component stress ratios. Currently, all components of the FSR have at least 40% margin in all components. A 10% increase in total stresses (conservatively including both RSA and transient analysis stresses) would increase the limiting ratio to an upper bound of 0.66 leaving 34% margin.

With the previous discussion in mind, there is not a concern that the small cross-correlation coefficient exceedances between time history inputs will result in component loads above their allowable values.

Finally, for reference, the NA3 synthesized acceleration time histories are shown in Figure 4, Figure 5, and Figure 6 for the plant North-South, East-West, and Vertical direction, respectively.

2.3 Results

The key findings from this reanalysis are documented in Table 1, Table 2, and Table 3 with comparisons to the corresponding results from the DCD. In general large reductions in displacements, forces, and stresses are seen as a result of using the NA3 site-specific SSE demands. This decrease is a result of the decrease in the horizontal spectra across all frequencies. The horizontal modes tend to dominate the component stresses for structures that are relatively rigid in the vertical direction such as the FSR. The effects of increased seismic demand in vertical direction for the spent fuel pool FSR is offset by the reduction in the horizontal direction.

Table 1 summarizes the enveloping maximum displacements and forces for the FSR obtained from the SSE time history analysis. The large decrease in displacement between the FSR foot and the pool floor confirms that there is no risk of the spent fuel pool FSR impacting the fuel pool wall. However, for

reference, this is confirmed by adding the thermal displacement to the maximum SSE displacement here:

The maximum displacement due to a seismic event is 2.7 mm in the North-South direction and 3.4 mm in the East-West direction (see Table 1). When combined with the thermal displacements resulting from a pool temperature of 121.1°C the maximum total displacements are:

North-South Total Displacement = 7.7 mm < 92 mm (North-South wall min distance)

East-West Total Displacement = 6.1 mm < 60 mm (East-West walls min distance)

As these displacements are less than the minimum horizontal distance to the pool walls, the FSR will not impact the walls.

Table 2 summarizes the critical stress results obtained from the analysis of the FSR and the comparison with the allowable values in accordance with the design code (Reference 7). All component stresses remain below their code allowable values and below the DCD results. The components of the spent fuel pool are structurally acceptable relative to the NA3 seismic demand.

Table 3 summarizes the enveloping maximum reactions on the bearing pad in the pool floor liner. All pool liner loads remain below their DCD results.

Table 1: Maximum Displacements and Forces Summary

	NEDO-33373 Rev. 5 Values (Table 1-2)		NA3 Specific Values	
Displacement/Force	**Horizontal**	**Vertical**	**Horizontal**	**Vertical**
Relative displacement between FSR foot and pool floor (mm)	39.5 (N-S direction) 36.1 (E-W direction)	26.0	2.5 (N-S direction) 3.2 (E-W direction)	1.6
Force by FSR foot between bearing pad and pool floor (kN)	Shear 1344	Compression 1843	Shear 736	Compression 1164
Relative horizontal displacement between FSR top and pool wall (mm)	39.5 (N-S direction) 48.9 (E-W direction)	-	2.7 (N-S direction) 3.4 (E-W direction)	-
Force between two FSRs at the lower link device (kN)	1306	-	728	-
Force between two FSRs at the upper link device (kN)	1227	-	433	-
Relative displacement between fuel and FSR (mm)	10 (at top)	3.7	10 (at top)	1.9
Force between fuel (all assemblies and FSR (kN)	1017 (at top) 814 (at bottom)	1708	331 (at top) 243 (at bottom)	1481
Global bending moment on the FSR base plate (kN*m)	1645 (E-W axis) 2176 (N-S axis)	-	1027 (N-S axis) 1434 (E-W axis)	-

Table 2: Fuel Storage Rack Main Stresses Summary Comparison

		NEDO-33373 Rev. 5 Values (Table 1-3)		NA3 Specific Values	
Steel Plates	**Stress Limit (MPa)**	**Stress (MPa)**	**Ratio**	**Stress (MPa)**	**Ratio**
10 mm thick Enveloping Plate	292.8	226	0.77	103	0.35
10 mm thick Enveloping Plate Welds	198.6	163	0.82	107	0.54
7 mm Thick Upper Level Plates	292.8	227	0.78	92	0.31
7 mm thick Upper Level Plate Welds	198.6	91	0.46	63	0.32
Fuel Support Base Plate	292.8	274	0.94	176	0.60
20 mm thick Base Plate Stiffener Plates	292.8	208	0.71	166	0.57
20 mm thick Base Plate Stiffener Plate Welds	198.6	136	0.68	99	0.50
Foot Cylindrical Nut	292.8	253	0.86	160	0.55
Foot Cylindrical Nut Welds	198.6	141	0.71	101	0.51
Nut Thread	198.6	107	0.54	68	0.34
Lower Links (Bearing Pad)	419.9	363	0.86	202	0.48
Upper Links (Assembly Crossarm)	1049.7	927	0.88	327	0.31

Table 3: Pool Liner Maximum Reactions

	NEDO-33373 Rev. 5 Values (Table 1-3a)	NA3 Specific Values
Shear (kN)	1398	866
Compression (kN)	1843	1782

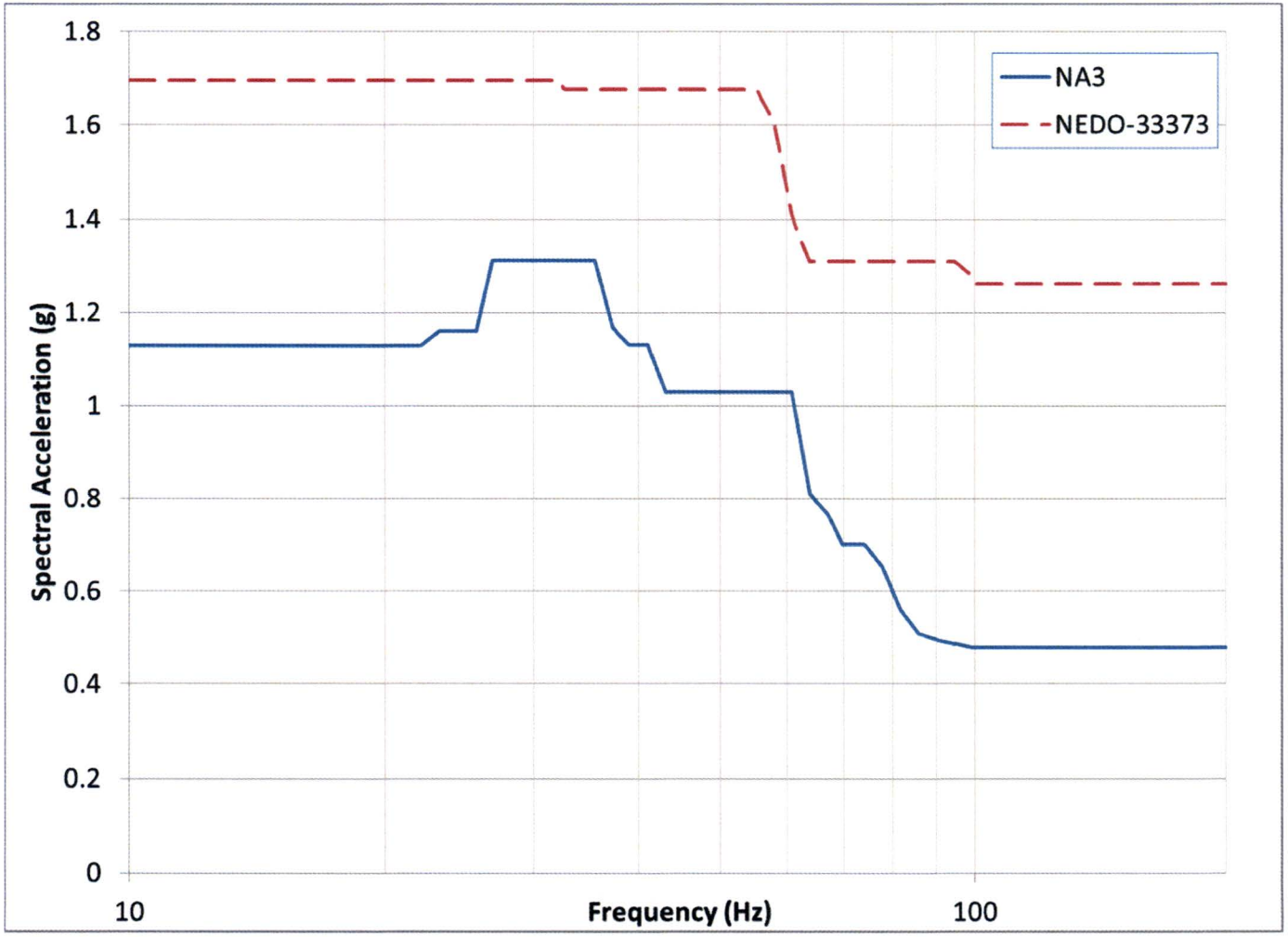

Figure 1: North-South Spent Fuel Pool FSR SSE Spectra Comparison (4% Damping)

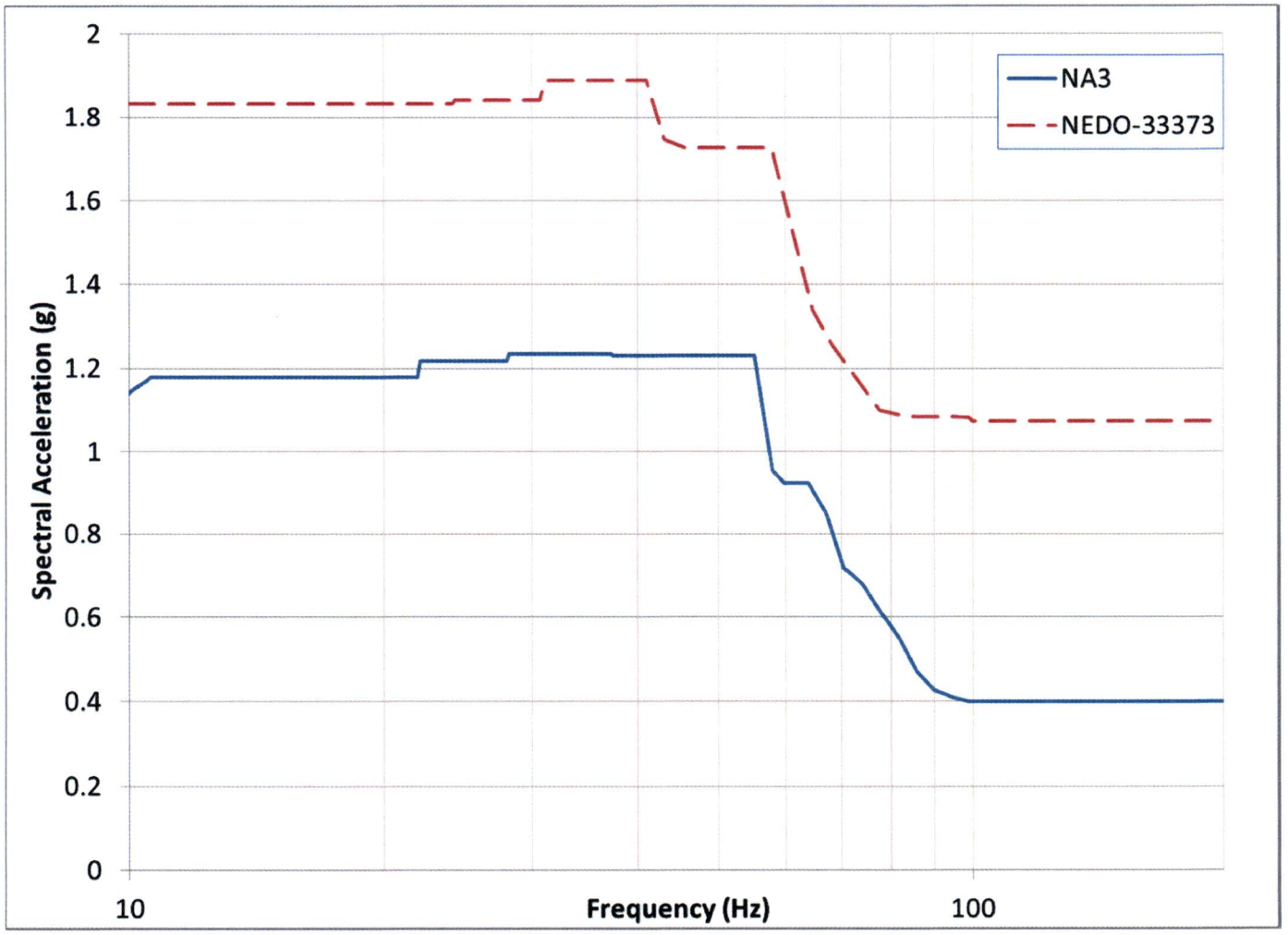

Figure 2: East West Spent Fuel Pool FSR SSE Spectra Comparison (4% Damping)

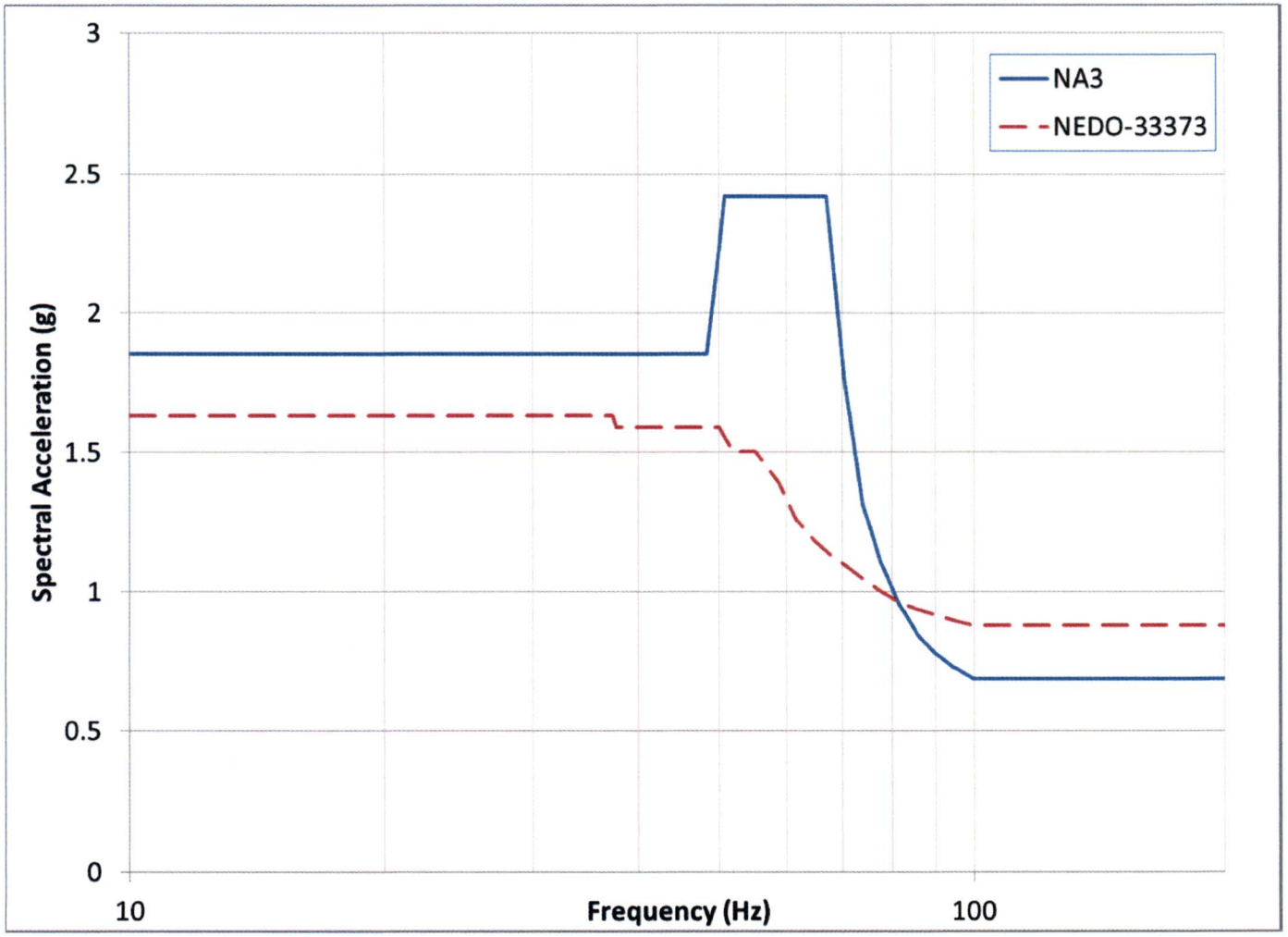

Figure 3: Vertical Spent Fuel Pool FSR SSE Spectra Comparison (4% Damping)

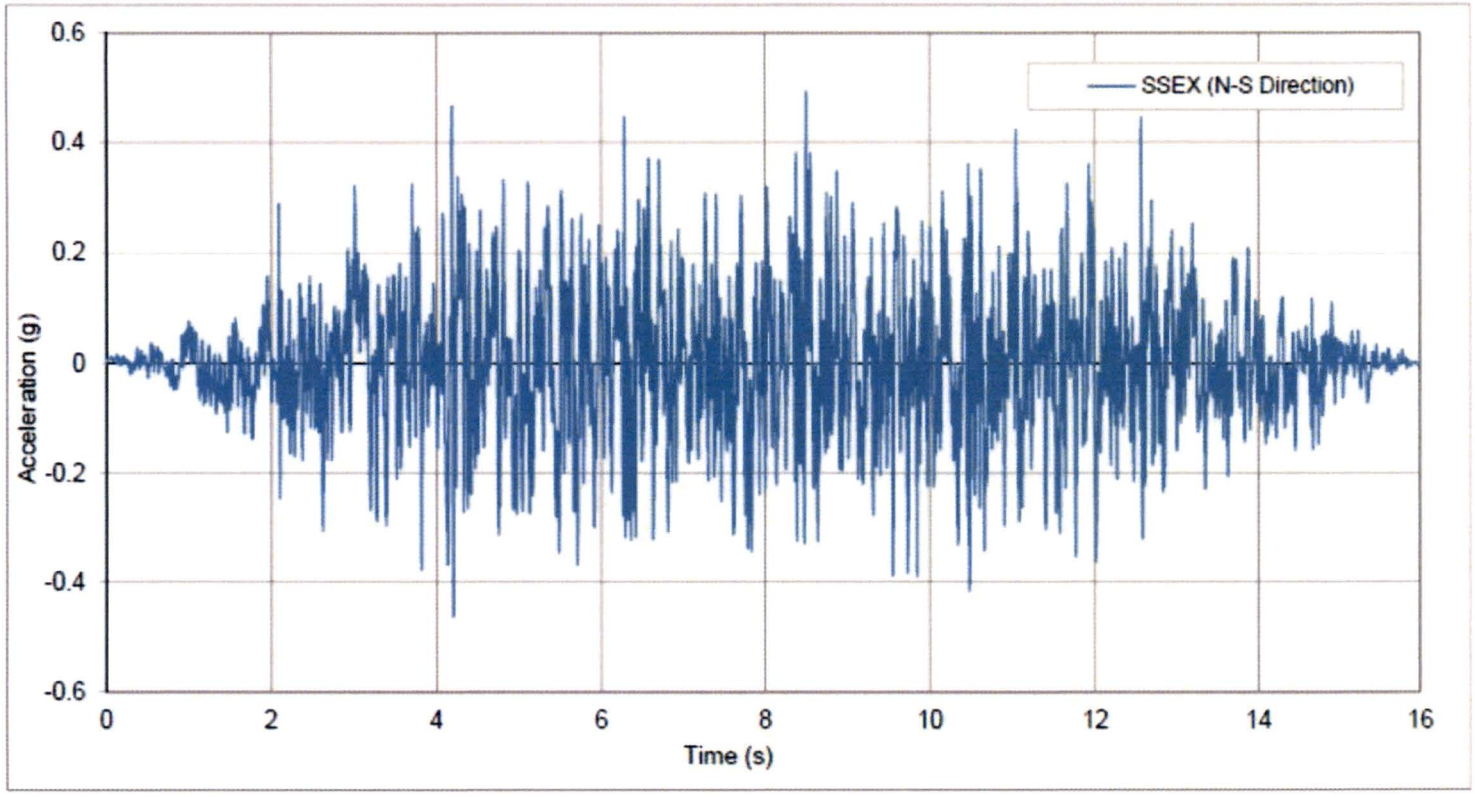

Figure 4: North-South Spent Fuel Pool FSR SSE Acceleration Time History

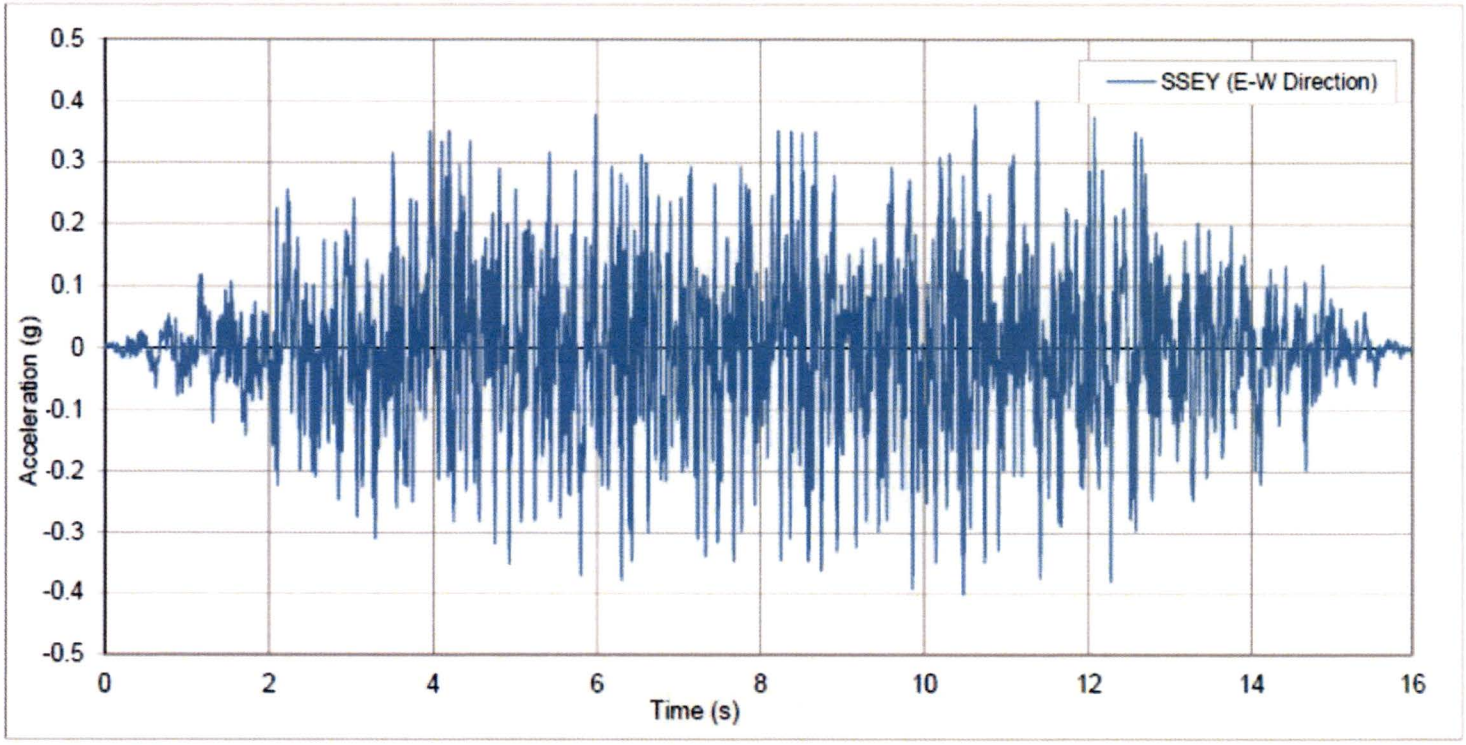

Figure 5: East-West Spent Fuel Pool FSR SSE Acceleration Time History

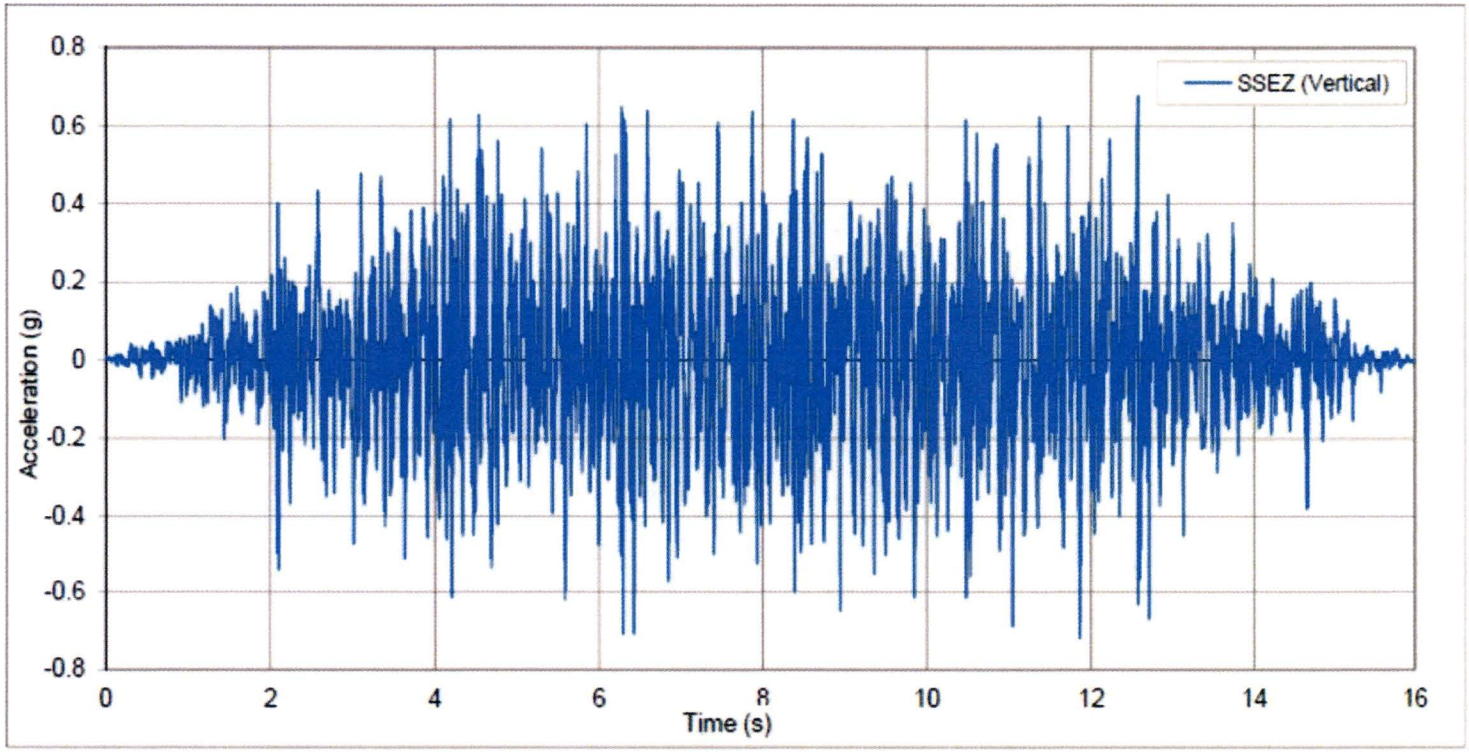

Figure 6: Vertical Spent Fuel Pool FSR SSE Acceleration Time History

3. SPENT FUEL RACKS IN THE BUFFER POOL DEEP PIT

The structural adequacy of the FSR in the buffer pool deep pit to the ESBWR DCD seismic demands was demonstrated in Section 2.0 of Reference 1. To ensure the structural adequacy of the FSR in the buffer pool deep pit for the seismic demands of NA3, the analysis documented in Section 2.0 of Reference 1 was repeated using the NA3 site-specific SSE acceleration response spectra. This analysis is contained in Reference 4.

A brief summary of the structural assessment is provided in Section 3.1. The information contained in Section 3.1 is a repeat of information provided in the ESBWR DCD buffer pool deep pit FSR report (Section 2.0 of Reference 1) as an aide in understanding the current, site-specific evaluation of these racks. The site-specific seismic demand for these racks is discussed in Section 3.2 along with a discussion of the response spectra used to generate time histories for the fuel impact evaluation. The maximum enveloping results of the assessment including stress results, displacements and anchorage embedment loads are provided in Section 3.3. Finally, the design changes to these racks to prevent overstressed components resulting from site-specific seismic demands are provided in Section 3.4.

3.1 Analysis Summary

The buffer pool deep pit FSR are qualified using guidance from Appendix D of SRP Chapter 3.8.4. The following is a brief description of the site-specific seismic evaluation of the buffer pool deep pit FSR. See Reference 4 for the assessment in its entirety.

Overview

The spent fuel racks in the buffer pool deep pit are designed to support and protect the spent fuel assemblies. They are made of stainless steel and borated stainless steel plates, forming 11x7 cells to house the spent fuel assemblies. The buffer pool deep pit FSR are anchored to the pool floor at the four bottom corner locations.

To analyze these racks both a RSA and transient analysis are performed to ensure the structural adequacy of the individual components responsible for maintaining the adequacy of the buffer pool deep pit FSR.

Design Code

The buffer pool deep pit FSR are designed to the stress limits of ASME B&PV Code, Section III, Division 1, Subsection NF requirements for Class 3 component supports (Reference 7).

Loads and Combinations

The only load combinations affected by the change in seismic demand is shown in Eq. (5) all other load combination results are unaffected by SSE loads.

Level D: $$D + SSE + SRVD + LOCA + T_a \quad (5)$$

The dead weight (D) is evaluated as a static load under the effect of gravity. The SSE, Safety Relief Valve Discharge (SRVD), and Loss-of-Coolant Accident (LOCA) are all dynamic loads acting at the base of the rack. There are no thermal (T_a) loads on the structure because sufficient clearance is provided for thermal expansion; however, the thermal displacement is considered in determining the potential impact with the pool wall.

Analysis Procedure

The analysis of the racks is divided into two calculation stages which both utilize the finite element program ANSYS 10.0. The structural adequacy of the buffer pool deep pit FSR to the static and building vibration loads is evaluated in a RSA. Additionally, the effect of fuel impacting the FSR during an SSE and the local stress qualification of the fuel base plate for this impact is evaluated in a non-linear transient analysis.

Analysis Procedure (RSA)

A detailed finite element model of a single buffer pool deep pit FSR is developed using shell and lumped mass elements. The deadweight loads are resolved by static analysis. The dynamic loads are resolved by RSA using first 100 modes up to 263.8 Hz. The site-specific response spectra are discussed in Section 3.2. Consistent with NRC Regulatory Gide 1.92, the modal responses for a given dynamic load in each direction are combined using the grouping method and the resulting spatial components are combined by Square root of the Sum of Squares (SRSS). The effects of missing mass in the RSA are accounted for using pseudo-static evaluation consistent with Appendix A of Reg. Guide 1.92.

The results of the RSA are used to determine the stresses in the buffer pool deep pit FSR components and the embedment loads to be used in the design of the embedment. In addition, the maximum displacements are combined with thermal displacements to ensure that the buffer pool deep pit wall is not impacted.

Analysis Procedure (Transient Analysis – Fuel Impact)

Synthesized site-specific acceleration time histories are converted to displacements by double integration and used as base input motion for simplified models representing the structural characteristics of the buffer pool deep pit FSR in the East-West and North-South direction. Each simplified model is composed of 2-D elastic beam elements representing the enveloping plate of the FSR and the fuel elements. The masses of the structures are lumped and hydrodynamic coupling is simulated between the fuel and the FSR. The fuel's lowest node is coupled to the FSR in the horizontal direction and a contact element is used in the vertical direction which allows the fuel to uplift and then impact the FSR. The fuel's uppermost node has horizontal contact elements to evaluate lateral impacts of the fuel with the FSR. This time history analysis was performed for 16 seconds using 0.005 second intervals. Section 3.2 contains additional information pertaining to the time history models used in the transient analysis as part of a discussion on the impact of potentially non-conservative time history inputs.

Maximum impact forces are obtained from the transient analysis found in Appendix C of Reference 4. These forces include the horizontal forces at the top and bottom of the fuel and vertical force at the bottom of the fuel. The stresses produced at the top of the fuel rack are negligible as the force at the top of the FSR is small (137 N). The stresses produced by the fuel forces on the base plate are analyzed by applying the impact loads (Vertical – 40,520 N, Horizontal 1,026 N) as nodal loads in three directions (max horizontal load applied in both horizontal directions) to the detailed model of the buffer pool deep pit FSR base plate. Due to the large vertical forces, a plastic stress-strain material curve is used and the stress is shown to be below the allowable value from Appendix F of the ASME Code.

3.2 Seismic Demand

The NA3 site-specific response spectra for the ESBWR fuel racks are provided in a site-specific design specification data sheet for the fuel racks (Reference 8). The NA3 response spectra for the spent fuel racks in the buffer pool deep pit documented in Reference 8 are the enveloped spectra from Node 106, 206, and 107 of the site-specific bounding SSE demands provided in Reference 9. Node 106 and 206 are located at the elevation of the base of the buffer pool deep pit with node 106 on the Reactor Building (RB) and 206 on the Reinforced Concrete Containment Vessel (RCCV). Node 107 is located on the deep pit wall on the RB at an elevation at which the input motion may be coupled to the FSR through the water in the pool and so its spectrum is conservatively included. All spectra for the fuel racks are taken at 4% damping consistent with Reg. Guide 1.61 for welded steel structures for SSE analysis.

The NA3 deep pit fuel FSR response spectra are shown with comparison to the equivalent DCD response spectra in Figure 7, Figure 8, and Figure 9 for the plant North-South, East-West and Vertical direction, respectively[3]. The DCD response spectra were retrieved from Section 2.0 of Reference 1.

The analysis of the spent fuel racks requires two synthesized acceleration time histories in addition to the response spectra. The time history is used in a non-

[3] The response spectra are provided from 10 Hz to 300 Hz as the fundamental frequency of the deep pit fuel racks is 13.6 Hz and the highest eigenvalue of the FSR calculated was 263.8 Hz.

linear transient analysis exclusively to determine the effect of fuel impact on the base plate during SSE. The time histories for this evaluation are shown in Figure 16 and Figure 17 for the horizontal and vertical direction, respectively. These time histories are discussed in Section 4.2 and were generated from the response spectra for the new FSR in the buffer pool.

The usage of the time histories from the higher elevation FSR in the buffer pool for the evaluation of the deep pit FSR represents a simplification of the analysis which eliminates the generation of additional time histories. The higher elevation's vertical response spectra bound that of the deep pit (Figure 10) but the higher elevation's horizontal response spectrum does not bound the horizontal response spectra of the deep pit in both horizontal directions (Figure 11). The spectral exceedances in the horizontal direction represent potential non-conservatisms in the corresponding time histories. The effect of these exceedances is discussed in the following section.

Horizontal Spectra Exceedance Evaluation

To assess the impact of the spectra used in the evaluation of the buffer pool deep pit FSR, the models used in the evaluation are discussed further here. As stated in Section 3.1, the North-South and East-West model each consist of two overlaid beams (shown on the following page as two separated beams for clarity) representing the fuel and the FSR enveloping plate/base. Each model is tuned to the approximate natural frequency of the detailed model in both horizontal directions. For both models, the fuel's lowest node is coupled to the FSR in the horizontal direction and a contact element is used in the vertical direction which allows the fuel to lift off the base plate and then return and impact the base plate. The fuel's uppermost node has horizontal contact elements used to evaluate lateral impacts of the fuel with the upper grid structure of the FSR.

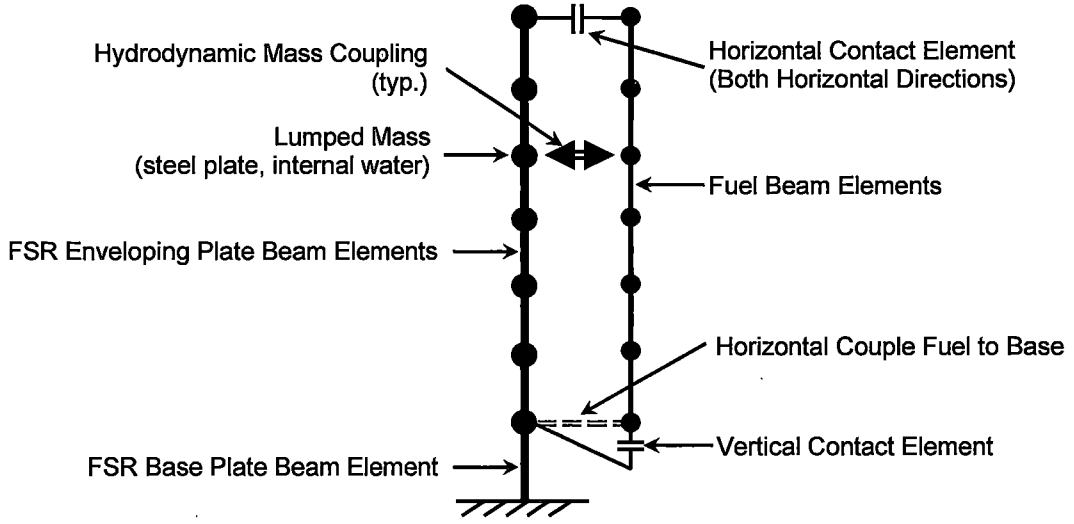

The fuel impact evaluation is performed by applying time histories in the vertical and horizontal direction as base input motion. This motion is transmitted through the FSR Base Plate element and into the fuel and the enveloping plate elements. Given that the fuel is free to rotate at the connection with the baseplate and is only constrained by displacement limitations at the top of the fuel, no moments are transferred from the rack to the fuel. The only inputs to the fuel motion are the horizontal impact at the top of the rack ($F_{H,T}$), horizontal reaction at the base plate ($F_{H,B}$) and the vertical reaction with the base plate (F_V)

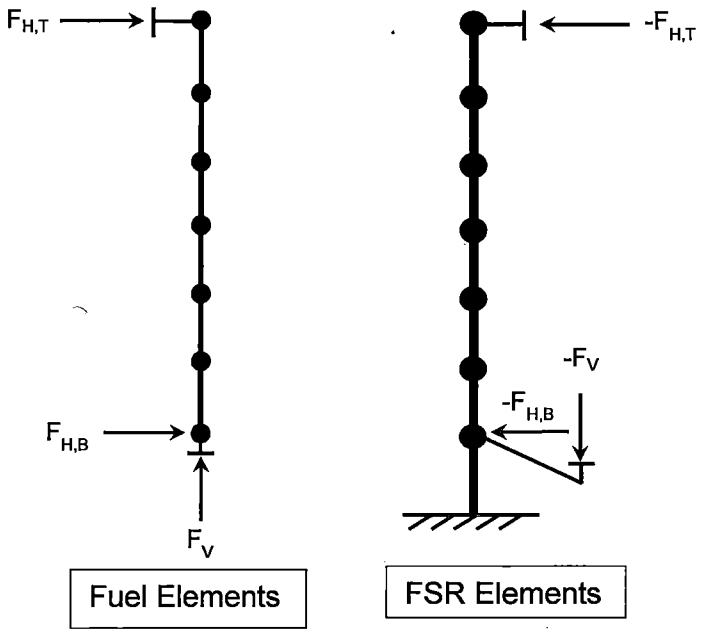

The stiffness matrix for a Euler-Bernoulli beam element in a two dimensional plane is given in Eq. (3). Notice that there is no coupling between the motion in the direction of the beam element (u) and the horizontal direction (v). However, if the fuel rotates sufficiently, stiffness components of the fuel would exist that couple the vertical response of the fuel to the horizontal input.

To estimate the amount of overturning in the fuel, θ_T, the maximum displacement of the fuel rack from the RSA (6.6 mm from Table 4) is added to the nominal gap between the fuel rack and the fuel (10 mm). The length of the fuel is roughly 3.5 m. Thus, for a maximum relative displacement of the fuel in the rack of 16.6 mm the angle of rotation of the fuel is small (≈0.3 degrees, see Eq. 6). Any transformation of the stiffness matrix by this angle would result in limited coupling between the horizontal input of the rack and the vertical response of the fuel. Additionally, as moments are not transferred from the fuel racks to the fuel, there is no coupling between the rotation of the FSR and the fuel's response. Thus, for this model, the vertical and horizontal responses can be considered practically decoupled.

$$\theta_T = tan^{-1}\left(\frac{0.0166\,m}{3.5\,m}\right) = 0.27° \qquad (6)$$

Given that the response of the model in the horizontal and vertical direction are almost entirely decoupled, any increase in the input in the horizontal direction will only act to increase the horizontal response of the fuel. Similarly, any change in the input in the vertical direction will only act to increase the response in the vertical direction. The horizontal loads acting on the deep pit FSR are roughly 40 times smaller than the vertical loads (40,520 N – Vertical vs 1,026 N – Horizontal – from Appendix C of Reference 4). To estimate the effect of the horizontal spectral exceedances, the maximum spectral exceedance was determined as a percentage and equals 76%[4]. The 76% spectral exceedance exists at 50 Hz where the required spectral acceleration is 2.02g compared to the 1.14g used in time history generation. A hypothetical increase of 76% in the horizontal loads accounting for the horizontal spectral exceedances would reduce the ratio of vertical to horizontal loads to 22 to 1.

[4] Horizontal spectral exceedances are below 40% except in the high frequency region between 43-62 Hz.

The horizontal loads are applied as in-plane loads on the plate which form local compressive stress fields in the area of the application while the vertical loads are applied as transverse loads on the plate which produce significant bending moments throughout the plate and the 22 to 1 ratio of vertical to horizontal loads will result in an even larger ratio of the resulting stresses. Given that a conservative vertical spectrum is being used and that the existing base plate impact analysis has a limiting stress of 206 MPa relative to an allowable of 436 MPa any non-conservatism in the horizontal time history can be considered negligible.

3.3 Results

The key findings from this reanalysis are documented in Table 4, Table 5, and Table 6 with comparisons to the corresponding results from the DCD. In general, there are increases in the stress and displacement results of roughly 15%-20%. The site-specific increases in the horizontal response spectra at low frequencies results in greater excitation of the low frequency structural modes that dominate the response of the FSR.

Due to the increase in the site-specific stresses on the FSR in the buffer pool resulted in overstressing the design of the anchor bolts and the 6 mm corner welds of the FSR. This is discussed in Section 3.4.

Table 4 summarizes the enveloping maximum horizontal displacement for the FSR obtained from the dynamic reanalysis. The maximum displacement has increased 1.1 mm from the DCD results. Given that the new maximum displacement is now 6.6 mm and the minimum distance to the nearest FSR or pool wall is 100 mm, there is not concern over an impact with a wall or an adjacent FSR.

Table 5 summarizes the critical stress results obtained from the analysis of the FSR and the comparison with the allowable values in accordance with the design code (Reference 7). All component stresses are below their code allowable values when the changes identified in Section 3.4 are incorporated.

Finally, Table 6 summarizes the enveloping maximum reactions on the bearing pad in the pool floor liner. The anchor embedment loads increased from the

DCD results. However, embedment design is outside the scope of this analysis and will be addressed later in the design process.

3.4 Design Changes

The site-specific evaluation of the FSR in the deep pit of the buffer pool resulted in the overstressing of the existing M48 anchor bolts and the corner filet welds attaching the 10 mm thick enveloping plate to the base stiffener plate (see Figure 12).

To accommodate the increase anchor loadings, the anchor bolts were switched from M48 to M52 bolts. The change in the size of anchor bolts does not affect the existing structural analysis as the bolt loadings are equivalent to the loading of the fixed nodes at the base of the FSR and thus, this design change has no effect on the structural qualification of the remaining FSR components.

The increase in the bending stresses at the weld from the 10 mm thick enveloping plate to the base stiffener plates resulted in the increase of the filet weld size from 6 mm to 8 mm at the corner locations. The change in this weld size does not affect the existing structural analysis as the weld size is not explicitly modeled. Instead, the stress is evaluated as the peak stress at the base of the enveloping plate corner multiplied by the ratio of the enveloping plate area to the weld area. See Figure 12 to review the location of the weld size changes.

The change in the anchor bolt and weld size do not invalidate the existing DCD structural adequacy evaluation (Reference 1) because the increase in size of both design changes result in lower stresses in these components and negligible change in stress in the other buffer pool deep pit FSR components.

Table 4: Maximum Buffer Pool FSR Displacements*

	NEDO-33373 Rev. 5 Values (Section 2.5.1)	NA3 Specific Values
Maximum Displacement (mm)	5.7	6.6

* Minimum distance between nearest FSR or pool wall is 100 mm

Table 5: Fuel Storage Racks Main Analysis Results

		NEDO-33373 Rev. 5 Values (Table 2-2)		NA3 Specific Values	
Steel Plates	**Stress Limit (MPa)**	**Stress (MPa)**	**Ratio**	**Stress (MPa)**	**Ratio**
10 mm thick enveloping plate	292.8	131	0.45	153.7	0.52
10 mm thick enveloping plate welds(1)	198.6	185.5	0.93	176.1(1)	0.90(1)
7 mm thick upper level plates	292.8	55.8	0.19	62.8	0.21
20 mm thick base plate	292.8	101	0.34	118	0.40
20 mm thick base plate stiffener plates	292.8	142	0.48	166	0.57
20 mm thick base plate stiffener plate welds	198.6	155.1	0.78	177	0.89
60 mm thick bolted support plates	292.8	174	0.59	200.1	0.68
Anchor Bolts(2)	1(3)	0.87(3)	0.87(3)	0.79(2),(3)	0.79(2),(3)

(1) Component design has changed from Reference 1. The filet size for the 10 mm thick enveloping plates has been updated from 6 mm to 8 mm due to a critical stress ratio of 1.06 for this component using the original weld design. See Section 3.1 for a discussion of this change.

(2) Component design has changed from Reference 1. M48x2 Anchor Bolts were changed to M52x2 Anchor Bolts due to a critical stress ratio of 1.12 using the original bolts. See Section 3.1 for a discussion of this change.

(3) This is a stress ratio, not a stress value.

Table 6: Anchor Bolt Embedment Loads[1]

	NEDO-33373 Rev. 5 Values (Table 2-13)	NA3 Specific Values
Level A Conditions Shear (N)	27665	27665
Level A Conditions Tensile (N)	54220[2]	54220[2]
Level D Conditions Shear (N)	396554	435233
Level D Conditions Tensile (N)	718507	841770

(1) As anchorages have not been specified, margins and allowable values are not included.

(2) Bolts do not withstand compression load in normal conditions

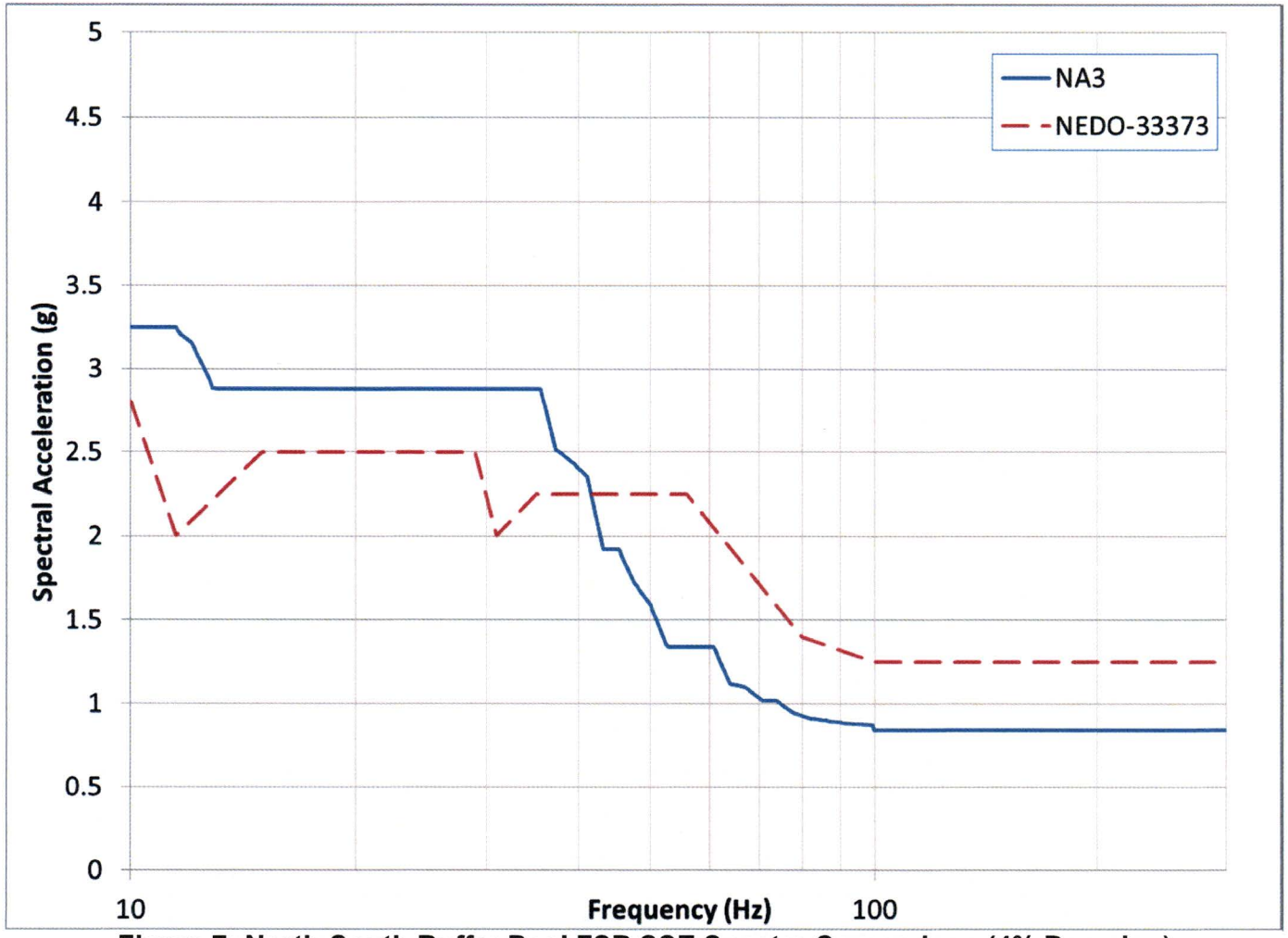

Figure 7: North-South Buffer Pool FSR SSE Spectra Comparison (4% Damping)

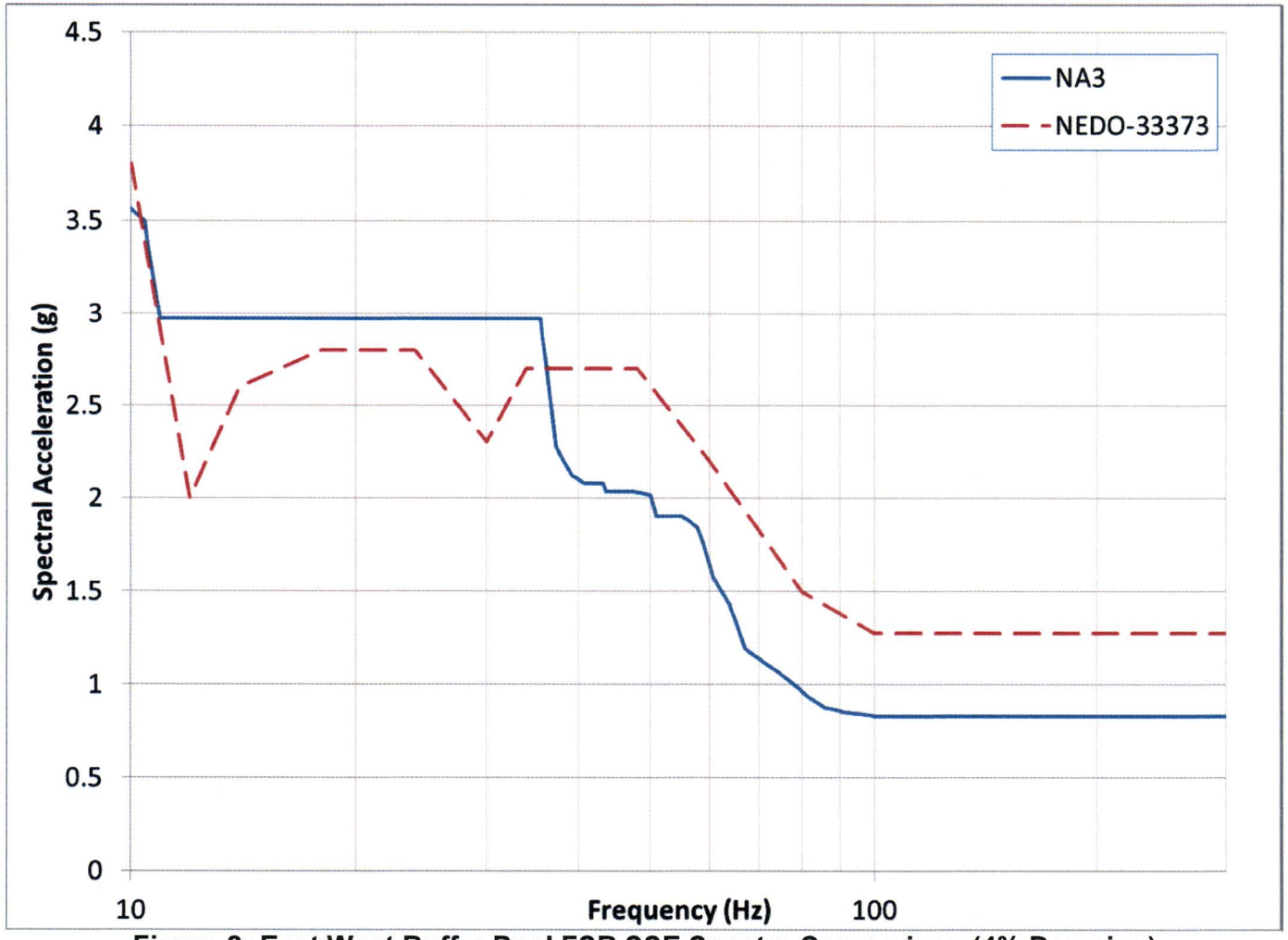

Figure 8: East West Buffer Pool FSR SSE Spectra Comparison (4% Damping)

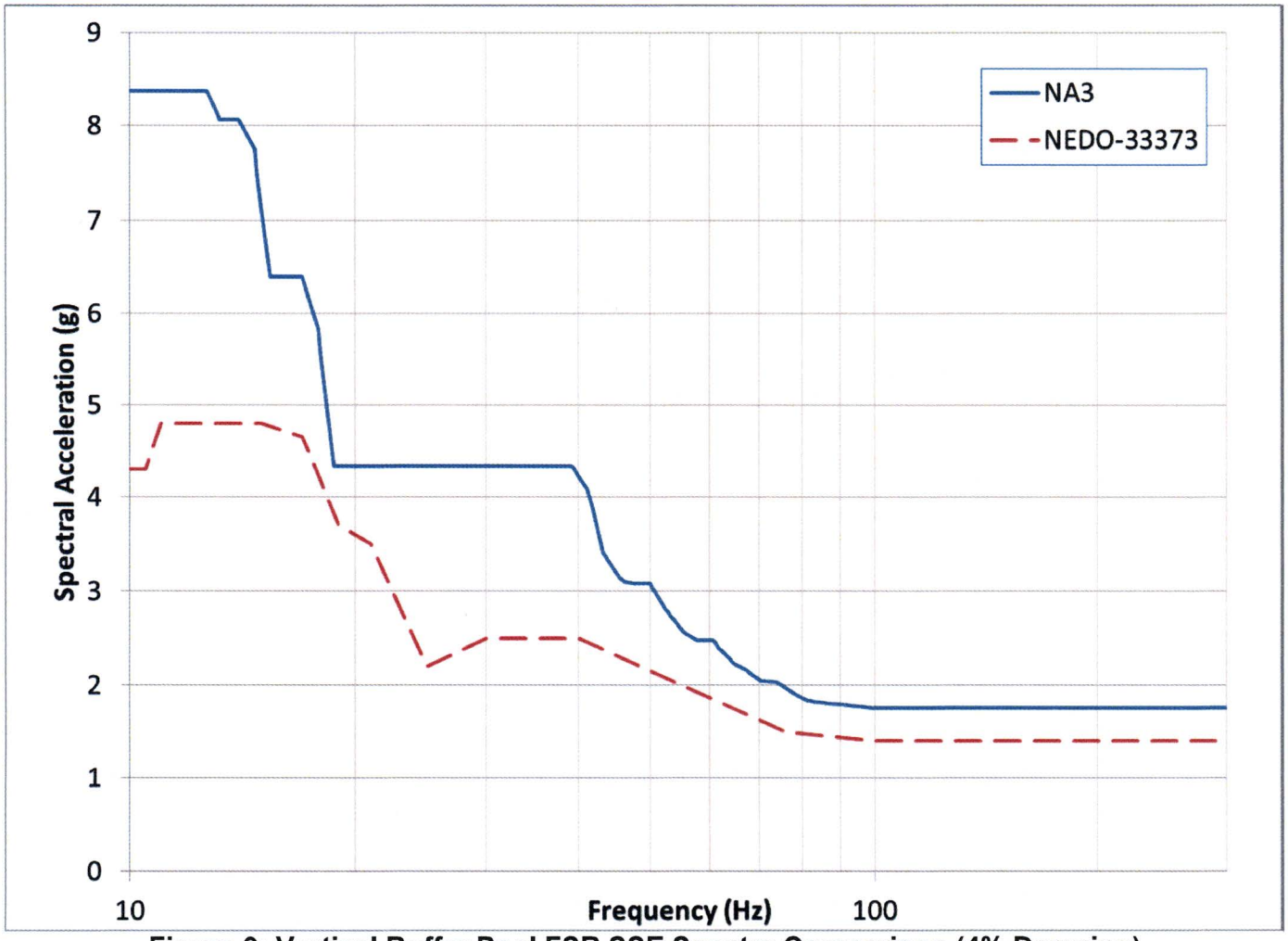

Figure 9: Vertical Buffer Pool FSR SSE Spectra Comparison (4% Damping)

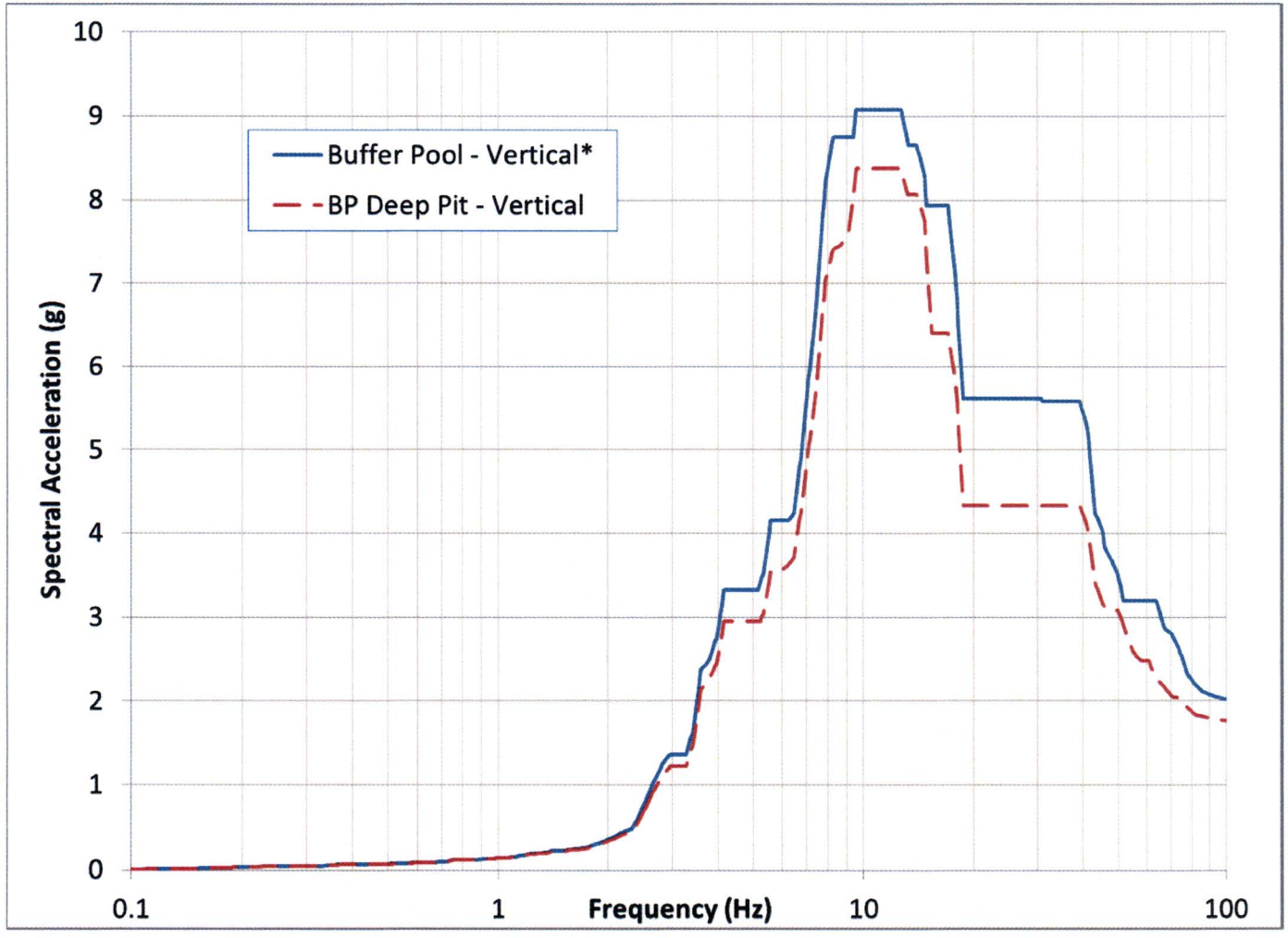

Figure 10: Comparison of Vertical Response Spectra for BP and BP Deep Pit

* Spectra used to generate time history for BP Deep Pit Fuel Impact Evaluation

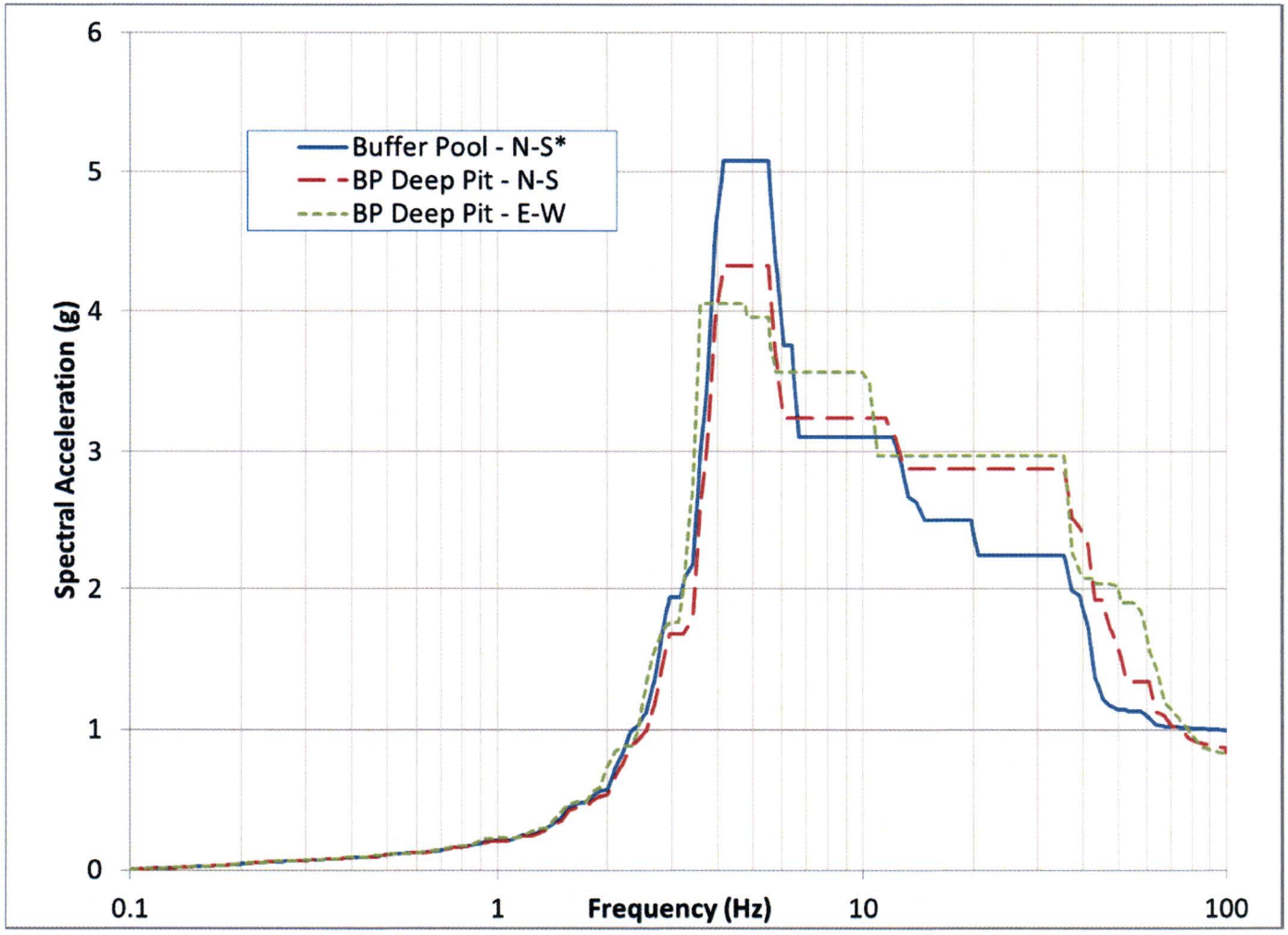

Figure 11: Comparison of Horizontal Response Spectra for BP and BP Deep Pit

* Spectra used to generate time history for BP Deep Pit Fuel Impact Evaluation

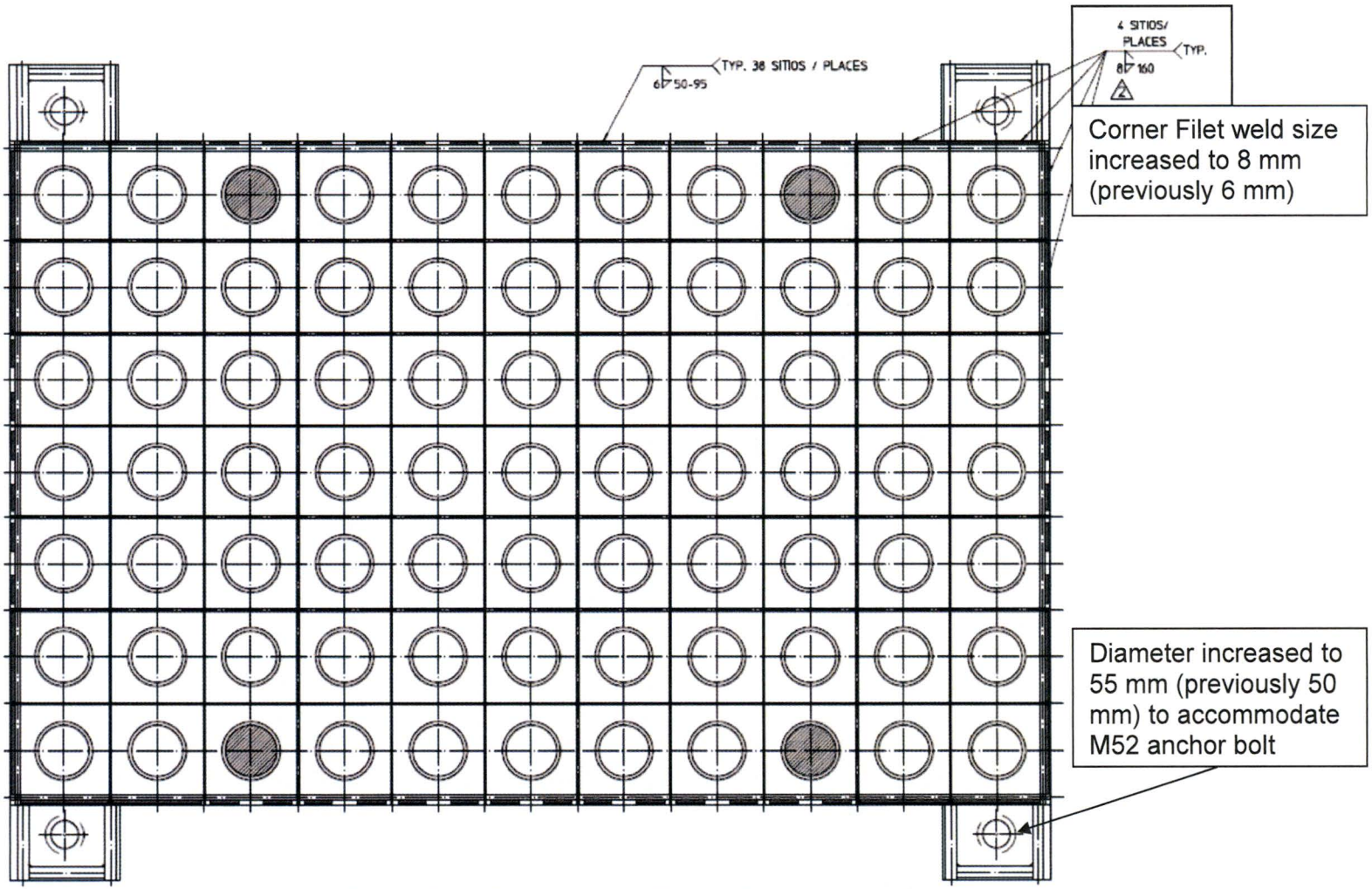

Figure 12: Spent Fuel Racks in the Buffer Pool Design Changes

4. NEW FUEL RACKS IN THE BUFFER POOL

The structural adequacy of the buffer pool new FSR to the ESBWR DCD seismic demands was demonstrated in Section 3.0 of Reference 1. To ensure the structural adequacy of the buffer pool new FSR for the seismic demands of NA3, the analysis documented in Section 3.0 of Reference 1 was repeated using the NA3 site-specific SSE acceleration response spectra. This analysis is contained in Reference 5.

A brief summary of the structural assessment is provided in Section 4.1. The information contained in Section 4.1 is a repeat of information provided in the ESBWR DCD buffer pool new FSR report (Section 3.0 of Reference 1) as an aide in understanding the current, site-specific evaluation of these racks. The site-specific seismic demand for these racks is discussed in Section 4.2. The maximum enveloping results of the assessment including stress results, displacements, and anchorage embedment loads are provided in Section 4.3. Finally, the design changes to these racks to prevent overstressed components resulting from site-specific seismic demands are provided in Section 4.4.

4.1 Analysis Summary

The buffer pool new FSR are qualified using guidance from Appendix D of SRP Chapter 3.8.4. The following is a brief description of the site-specific seismic evaluation of the buffer pool new FSR. See Reference 5 for the assessment in its entirety.

Overview

The new fuel storage racks in the reactor building buffer pool are designed to support and protect new fuel assemblies. They are made of stainless steel plates, forming 7x2 cells each cell housing a new fuel assembly. Two new FSR are joined and installed together forming a 14x2 configuration. The new FSR are anchored to floor of the buffer pool at several locations along their length.

To analyze these racks both a RSA and transient analysis are performed to ensure the structural adequacy of the individual components responsible for maintaining the adequacy of the buffer pool new FSR.

Design Code

The buffer pool new FSR are designed to the stress limits of ASME B&PV Code, Section III, Division 1, Subsection NF requirements for Class 3 component supports (Reference 7).

Loads and Combinations

The only load combination affected by the change in seismic demand is shown in Eq. (7) all other load combination results are unaffected by SSE loads.

Level D: $$D + SSE + SRVD + LOCA + T_a \quad (7)$$

The dead weight (D) is evaluated as a static load under the effect of gravity. The SSE, Safety Relief Valve Discharge (SRVD), and Loss-of-Coolant Accident (LOCA) are all dynamic loads acting at the base of the rack. There are no thermal (T_a) loads on the structure because sufficient clearance is provided for thermal expansion; however, the thermal displacement is considered in determining the potential impact with the pool wall.

Analysis Procedure

The analysis of the new FSR is divided in to two calculation stages which both utilize the finite element program ANSYS 10.0. The structural adequacy of the buffer pool deep pit FSR to the static and vibration loads is evaluated by RSA Additionally, the potential for the fuel rack to impact during an SSE and the local stress qualification of the fuel base plate for this impact is evaluated in a non-linear transient analysis.

Analysis Procedure (RSA)

A detailed finite element model of joined buffer pool new FSR set (14x2 cells) is developed using shell and lumped mass elements. The deadweight loads are resolved by static analysis. The dynamic loads are resolved by RSA using the first 150 modes up to 81.63 Hz. The site-specific response spectra are

discussed in Section 4.2. Consistent with NRC Regulatory Guide 1.92 Revision 1, the modal responses for a given dynamic load in each direction are combined using the grouping method and the resulting spatial components are combined by SRSS. The effects of missing mass in the RSA are accounted for using pseudo-static evaluation consistent with Appendix A of Reg. Guide 1.92.

The results of the RSA analysis are used to determine the stresses in the buffer pool new FSR components and the embedment loads to be used in the design of the embedment. In addition, the maximum displacements are combined with thermal displacements to ensure that the buffer pool deep pit wall is not impacted.

Analysis Procedure (Transient Analysis – Fuel Impact)

Synthesized site-specific acceleration time histories are converted to displacements by double integration and used as base input motion for simplified models representing the structural characteristics of the buffer pool new FSR in the East-West and North-South direction. Each simplified model is composed of 2-D elastic beam elements representing the enveloping plate of the FSR and the fuel elements. The masses of the structures are lumped and hydrodynamic coupling is simulated between the fuel and the FSR. The fuel's lowest node is coupled to the FSR in the horizontal direction and a contact element is used in the vertical direction which allows the fuel to uplift and then impact the FSR. The fuel's uppermost node has horizontal contact elements to evaluate lateral impacts of the fuel with the FSR. This time history analysis was performed for 16 seconds using 0.005 second intervals.

Maximum impact forces are obtained from the transient analysis in Appendix C of Reference 5. These forces include the horizontal forces at the top and bottom of the fuel and the vertical impact force at the bottom of the fuel. The stresses produced at top of the fuel rack are negligible as the force at the top of the FSR is small (692 N). The stresses produced by the fuel forces on the base plate are analyzed by applying the fuel's lower loads (Vertical – 60,714 N, Horizontal 2,221 N) as nodal loads in three directions (maximum horizontal applied in both horizontal directions) to the detailed model of the deep pit FSR used for the RSA. Due to the large vertical forces, a plastic stress-strain material curve is used and

the stress is shown to be below the allowable value from Appendix F of the ASME Code.

4.2 Seismic Demand

The NA3 site-specific response spectra for the ESBWR fuel racks are provided in a site-specific design specification data sheet for the fuel racks (Reference 8). The NA3 response spectra for the buffer pool new FSR documented in Reference 8 are the enveloped spectra from the following nodes from the site-specific bounding SSE demands provided in Reference 9.

X-Direction: Node 108 and 208

Y-Direction: Node 108 and 208

Z-Direction: Node 108, 208, 9081, 9082, 9085, and 9086

Node 108 and 208 are at the elevation of the bottom of the buffer pool with node 108 on the Reactor Building and node 208 on the RCCV. The additional nodes in the vertical direction are vertical slab oscillators that represent additional motion resulting from floor flexibility. All spectra for the fuel racks are taken at 4% damping consistent with Reg. Guide 1.61 for welded steel structures for SSE analysis.

The NA3 buffer pool new FSR response spectra are shown with comparison to the equivalent DCD response spectra in Figure 13, Figure 14 and Figure, 15 for the plant North-South, East-West and Vertical direction respectively[5]. All DCD responses were retrieved from Section 3.0 of Reference 1.

The analysis of the new FSR requires a synthesized acceleration time histories in addition to the response spectra. The time history is used in a non-linear transient analysis to determine the fuel impact forces occurring after fuel uplift

[5] The response spectra are provided from 1 to 100 Hz as the fundamental frequency of the buffer pool new FSR is 7.2 Hz and the highest eigenvalue of the FSR calculated was 81.6 Hz.

has occurred during an SSE event. The synthesized acceleration time histories for the buffer pool new FSR are documented in Reference 12. Reference 12 demonstrates that the response spectra generated in each direction sufficiently envelops the design spectra and that the cross-correlation coefficient between the resulting time histories is 0.14 which is below the SRP Section 3.71 requirement.

The NA3 synthesized acceleration time histories are shown in Figure 16 and Figure 17 for the horizontal and vertical direction, respectively.

4.3 Results

The key findings from this reanalysis are documented in Table 7, Table 8, and Table 9 with comparisons to the corresponding results from the DCD. There is slight increase in the stresses and displacements of some, but not all, of the components. This is primarily due to the horizontal site-specific spectra exceedances at the natural frequency of the structure (7.2 Hz).

The increase in the site-specific stress on the buffer pool new FSR resulted in the overstressing of the anchor bolts. The increase in the diameter of these bolts is discussed in Section 4.4.

Table 7 summarizes the enveloping maximum horizontal displacement for the new FSR obtained from the dynamic reanalysis. The maximum horizontal displacement has increased 3 mm from the DCD results; however, the site-specific maximum displacement (24 mm) is still well below the minimum distance to the nearest rack or wall (100 mm). There is no concern about the new FSR impacting either adjacent racks or the pool wall.

Table 8 summarizes the enveloping critical stress results obtained from the analysis of the new FSR and the comparison with the allowable values in accordance with the design code. All component stresses remain below their code allowable values when the design change identified in Section 4.4 has been incorporated.

Table 9 summarizes the enveloping maximum reactions on the bearing pad in the pool floor liner. The Level D anchor embedment shear load has decreased from the DCD results while the tensile load has increased. The increased loads on the embedment will be accounted for in the future work of designing the buffer pool new FSR bolt embedment.

4.4 Design Changes

The site-specific evaluation of the NFSR in the buffer pool resulted in the overstressing of the existing M24 anchor bolts.

To accommodate the increase anchor loadings, the anchor bolts were switched from M24 to M27 bolts. The existing design of the rack had enough room to accommodate this increase in the bolt size and so no changes were made to the rack itself. The change in the size of anchor bolts does not affect the existing structural analysis as the bolt loadings are equivalent to the loading of the fixed nodes at the base of the FSR and thus, this design change has no effect on the structural qualification of the remaining components.

The change in the anchor bolt size does not invalidate the existing DCD structural adequacy evaluation (Reference 1) because the increase in size would result in lower stresses in the bolts with negligible change in the buffer pool new FSR component stresses.

Table 7: Maximum Buffer Pool NFSR Displacements*

	NEDO-33373 Rev. 5 Values (Section 3.5.1)	NA3 Specific Values
Maximum Displacement (mm)	21.0	23.96

* Minimum distance between FSR and pool wall is 100 mm

Table 8: NFSR Main Analysis Results

		NEDO-33373 Rev. 5 Values (Table 3-2)		NA3 Specific Values	
Steel Plates	**Stress Limit (MPa)**	**Stress (MPa)**	**Ratio**	**Stress (MPa)**	**Ratio**
8 mm thick channel plate	292.8	267	0.91	197	0.67
Channel to support-base welds	198.6	182	0.92	185.3	0.93
12 mm thick door plates	195.2	123	0.63	145	0.74
Assembly grid plate	195.2	52.5	0.27	43.9	0.23
Axis and hinge	195.2	130	0.67	152.8	0.78
15 mm thick support-base stiffeners	195.2	138	0.71	155	0.79
15 mm thick folded base plate	292.8	266	0.91	247	0.84
30 mm thick bolted support plates	292.8	124	0.42	144	0.49
Anchor Bolts[1]	1[2]	0.91[2]	0.91[2]	0.62[1],[2]	0.62[1],[2]

(1) Component design has changed from Reference 1. M24x2 Anchor Bolts were changed to M27x2 Anchor Bolts due to a critical stress ratio of 1.03 using the original bolts. See Section 4.1 for a discussion of this change.

(2) This is a stress ratio, not a stress value.

Table 9: Anchor Bolt Embedment Loads[1]

	NEDO-33373 Rev. 5 Values (Table 3-15)	NA3 Specific Values
Level A Conditions Shear (N)	5390	5390
Level A Conditions Tensile (N)	2239[2]	2239[2]
Level D Conditions Shear (N)	93701	77771
Level D Conditions Tensile (N)	218410	254340

(1) As anchorages have not been specified, margins and allowable values are not included.

(2) Bolts do not withstand compression load in normal conditions

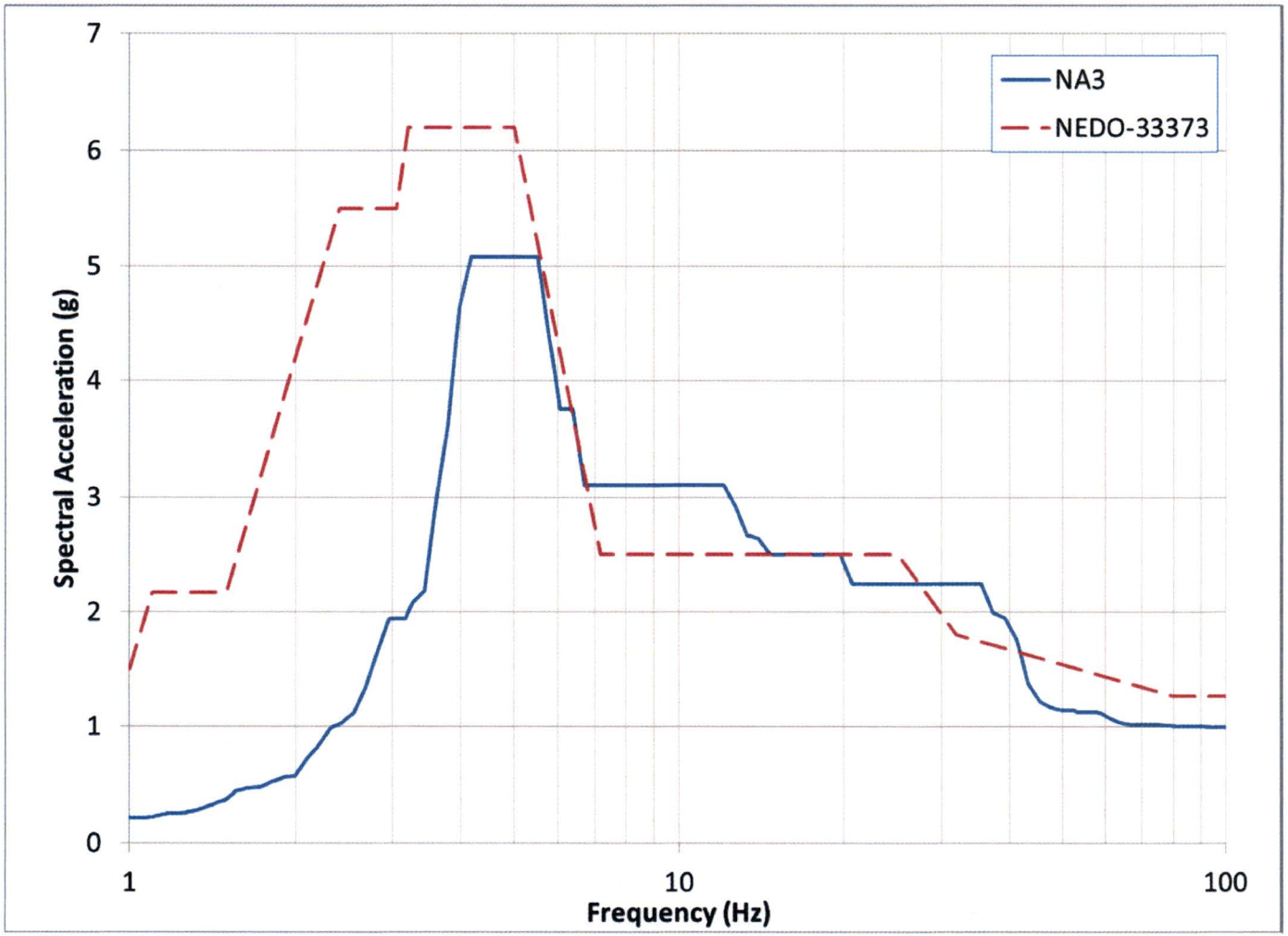

Figure 13: North-South Buffer Pool New Fuel Rack SSE Spectra Comparison (4% Damping)

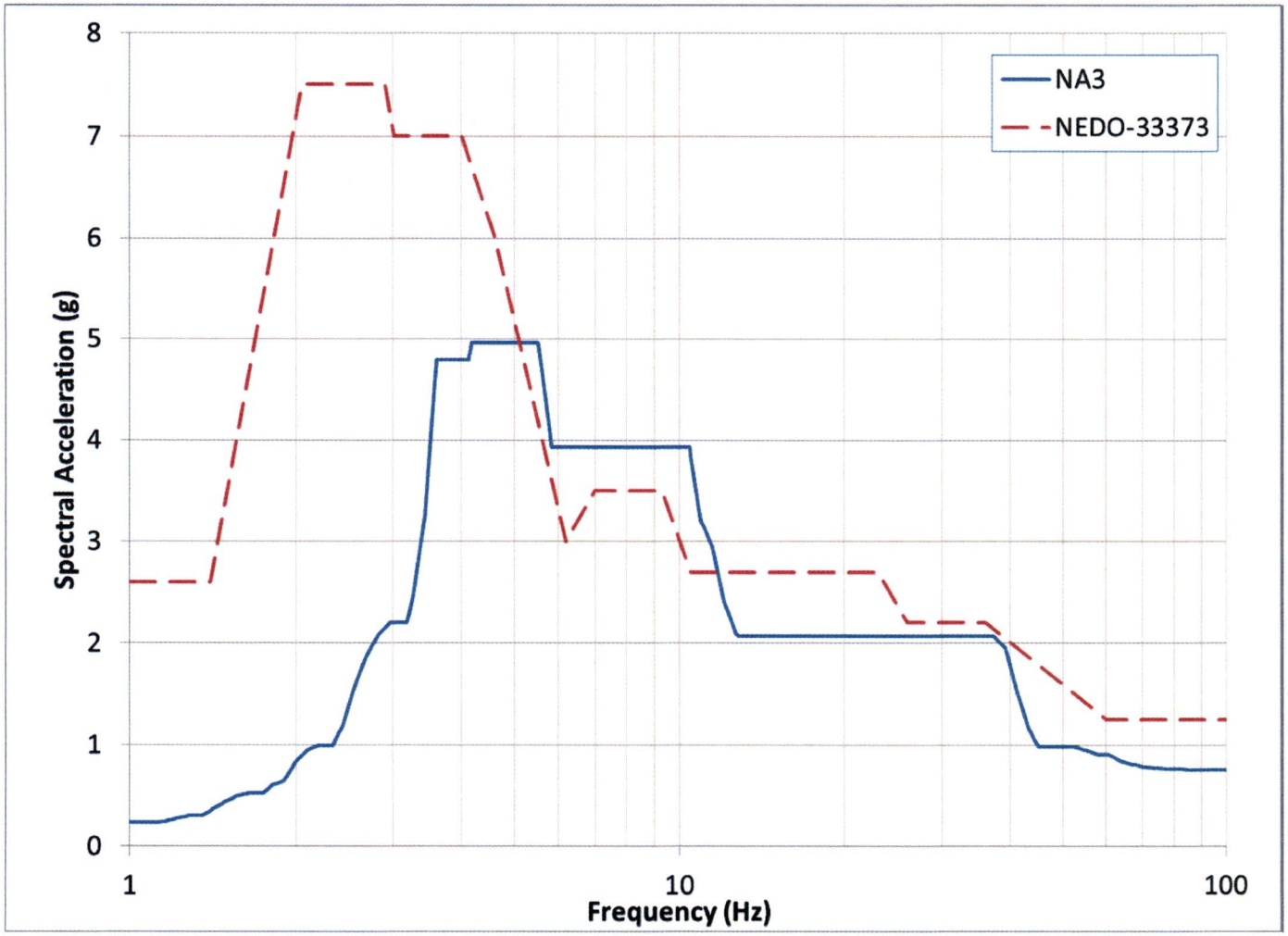

Figure 14: East-West Buffer Pool New Fuel Rack SSE Spectra Comparison (4% Damping)

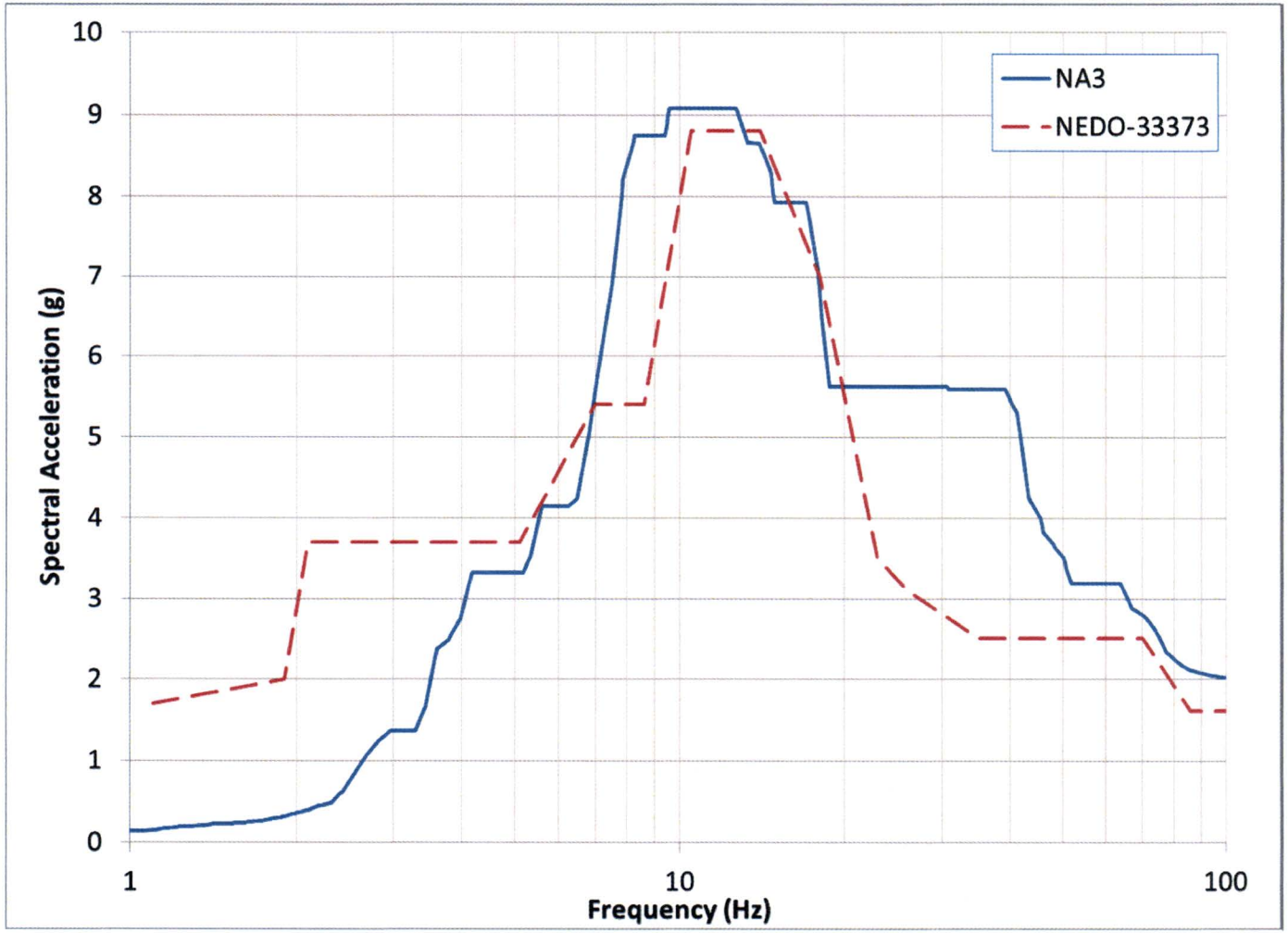

Figure 15: Vertical Buffer Pool New Fuel Rack SSE Spectra Comparison (4% Damping)

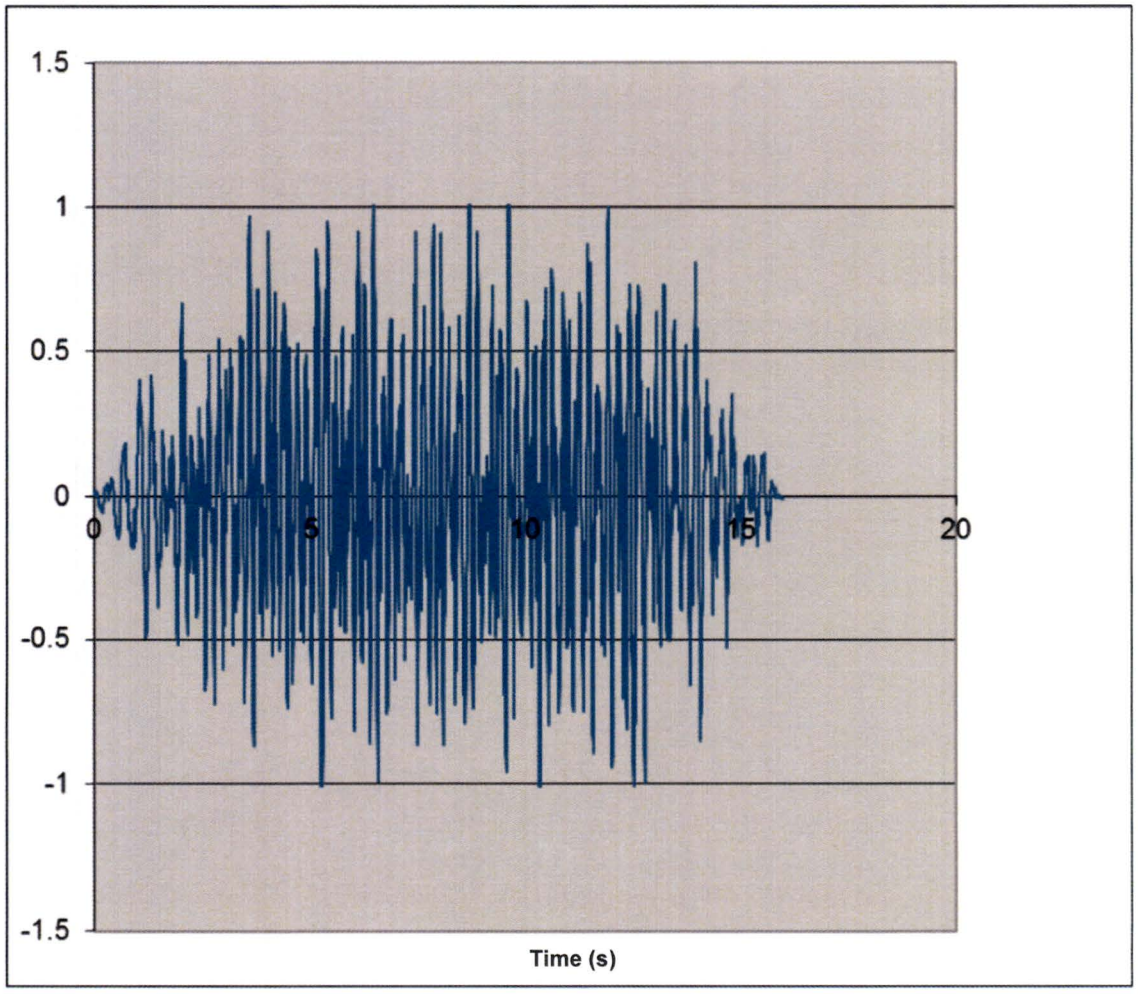

Figure 16: Horizontal Buffer Pool FSR SSE Acceleration Time History (Units: g)

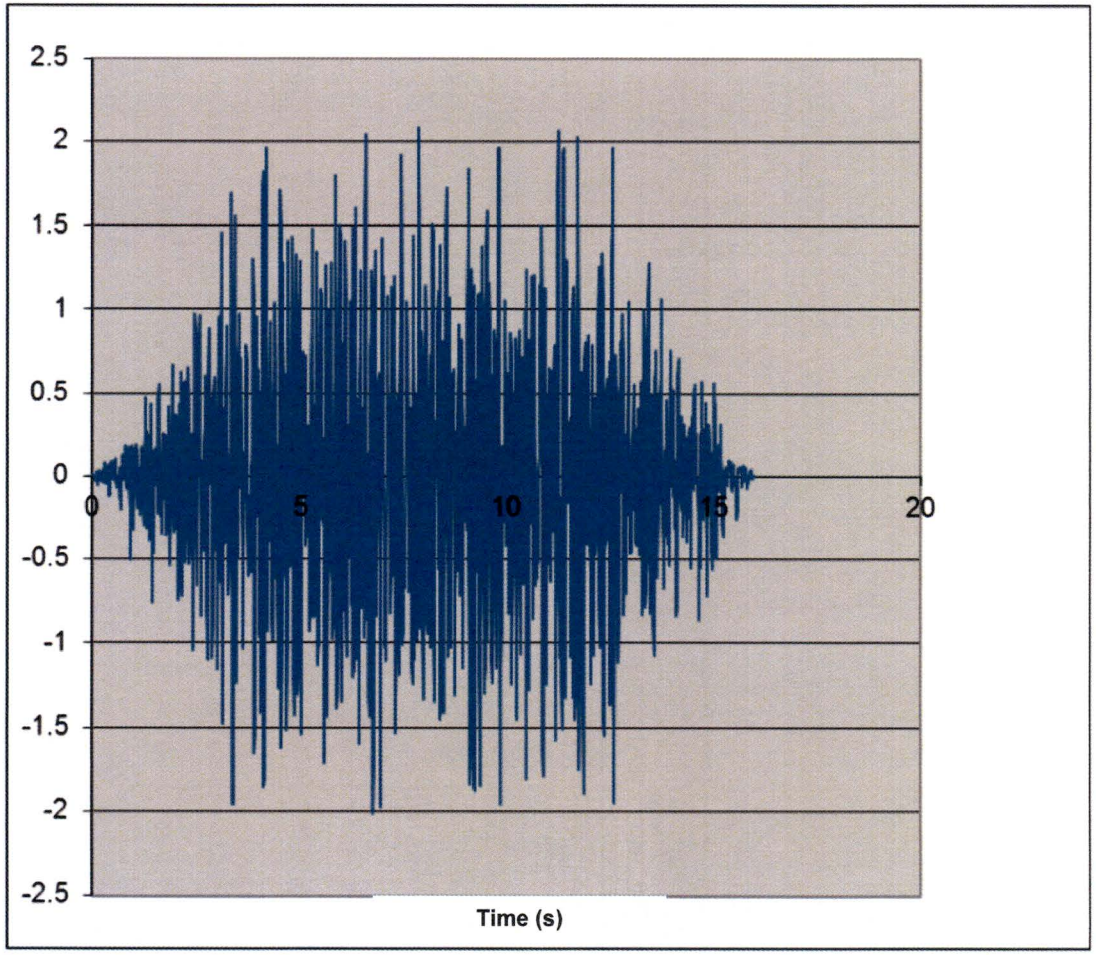

Figure 17: Vertical Buffer Pool FSR SSE Acceleration Time History (Units: g)

5. CONCLUSION

Using methodologies identical to those used in the ESBWR Licensing Topical Report (Reference 1), the fuel storage rack designs were re-evaluated using NA3 site-specific SSE acceleration response spectra.

The re-evaluation showed:

1. The spent fuel storage racks in the spent fuel pool had decreases in maximum displacements, stresses and pool reaction loads, demonstrating the adequacy of the design of these racks for NA3 seismic demands.

2. The spent fuel storage racks in the buffer pool deep pit required increases to the size of the anchor bolts and the welds from the enveloping plate to the base plates due to NA3 seismic demands. The NA3 embedment loads increased which will be accommodated during final embedment design.

3. The new fuel storage racks in the buffer pool required an increase to the size of the anchor bolts due to NA3 seismic demands. The NA3 embedment loads increased which will be accommodated during final embedment design.

Although the NA3 site-specific fuel rack seismic analysis concludes that the response spectra of the ESBWR DCD is not bounded across all frequencies and requires design changes for NA3, these changes do not invalidate the seismic qualification of the standard ESBWR plant design as described in Reference 1 because they result in lower component stresses.

6. REFERENCES

1) NEDO-33373 Rev. 5, "Dynamic, Load-Drop and Thermal-Hydraulic Analyses for ESBWR Fuel Racks", September 2010.

2) North Anna 3, Docket Number 52-017, Request for Additional Information 123, July 2014.

3) Document # 092-322-F-M-00001 Rev. 1 "Design Report of the Spent Fuel Storage Racks in the Fuel Building for North Anna 3," June 2015.

4) Document # 092-322-F-M-00003 Rev. 1 "Design Report of the Spent Fuel Storage Racks in the Reactor Building for North Anna 3," June 2015.

5) Document # 092-322-F-M-00002 Rev. 2 "Design Report of the New Fuel Storage Racks in the Reactor Building for North Anna 3," June 2015.

6) GEH Document # 003N0526 Rev. 1, "North Anna 3 Seismic Qualification of Spent Fuel in the Spent Fuel Racks," October 2015.

7) ASME Boiler and Pressure Vessel Code, Section III Rules for Construction of Nuclear Facility Components, Division 1, Subsection NF, Supports, 2001 Edition with Add. 2003.

8) GEH Document # 26A7032AA, "Fuel Storage Rack Design Specification Data Sheet," April 2015.

9) Document # SER-DMN-019 Rev. 1, "RB/FB Seismic Analyses Bounding Results and In-Structure Response Spectra," April 2015.

10) Document # 5926ATN02 Rev. 3, "ESBWR Fuel Building Pool Bottom Synthesized SSE Acceleration Time Histories," October 2015.

11) Pilkey, W. D. (2005). *Formulas for Stress, Strain, and Structural Matrices* (2nd Edition).

12) Document # 5926ATN04 Rev. 2, "ESBWR Reactor Pool Bottom (elevation +27 m) Synthesized SSE Acceleration Time Histories," October 2015.